

27 MAY 1948

NATIONAL ADVISORY COMMITTEE FOR AERONAUTICS

TECHNICAL NOTE

No. 1576

WIND-TUNNEL INVESTIGATION OF A SYSTEMATIC SERIES OF
MODIFICATIONS TO A FLYING-BOAT HULL

By Felicien F. Fullmer, Jr.

Langley Memorial Aeronautical Laboratory
Langley Field, Va.



Washington
May 1948

FOR REFERENCE

NOT TO BE TAKEN FROM THIS ROOM

N A C A LIBRARY
LANGLEY MEMORIAL AERONAUTICAL
LABORATORY
Langley Field, Va.

NATIONAL ADVISORY COMMITTEE FOR AERONAUTICS

TECHNICAL NOTE NO. 1576

WIND-TUNNEL INVESTIGATION OF A SYSTEMATIC SERIES OF
MODIFICATIONS TO A FLYING-BOAT HULL

By Felicien F. Fullmer, Jr.

SUMMARY

An investigation was conducted to determine, for one representative hull form, the effect on some of the aerodynamic characteristics of systematic variations in the shape and disposition of the chines at and near the bow and in the depth of the step. The parent hull was of conventional design (length-beam ratio equal to 6.7) and had a depth of step equal to 8 percent of the beam. The investigation was conducted at a Reynolds number of 6.4×10^6 based on the model hull length and all the tests were made with the hull attached to a wing which completely spanned the tunnel.

An analysis of the results obtained at an angle of trim which corresponded to the assumed high-speed attitude of the hulls ($\tau = -0.2^\circ$) showed that the drag coefficient based on hull frontal area of the "parent" hull was 0.090. Although the variations in the lines of the bow in general had only a small effect on the drag coefficient of the hull, a reduction in drag equal to 9 percent of the drag of the parent hull could be obtained by using a slender bow (profile view) incorporating a chine faired to conform more closely to the direction of the air flow at the bow. The drag coefficient for the hull with deep steps, 12 to 16 percent of the beam, was the same as that for the parent hull. The drag coefficient for the hull with a step depth equal to 4 percent of the beam was 20 percent less than that for the parent hull; and complete elimination of this step, except for the chine flare, produced no further reduction in the drag. A compromise arrangement consisting of an auxiliary longitudinal step and a shallow transverse step (4 percent of the beam) produced a hull which had 14 percent less drag than that of the parent hull and was believed to be hydrodynamically practical. Rounding a part of the forebody or afterbody chines of the parent hull, either separately or together, produced the same (18 percent) decrease in the drag coefficient. The elimination of the sharp chines, the step, and the small discontinuity caused by the forebody chine flare reduced the drag coefficient of the parent hull by about 30 percent. One-third of this total reduction in drag is attributable to the elimination of the sharp chines whereas the remaining two-thirds is due to the elimination of the step.

INTRODUCTION

The aerodynamic drag of hulls is an exceedingly important factor in the design of flying boats because of its influence on the parameters which determine the range and pay load and also because this drag has an important effect upon the maximum speed. For this reason, investigations of large scope have been conducted by the National Advisory Committee for Aeronautics to determine the drag reductions that can be obtained by the aerodynamic refinement of flying-boat hulls. Some of these investigations previously reported included tests of conventional hulls of length-beam ratios from 6 to 15 (reference 1), tests of planing-tail hulls developed by the NACA (reference 2), and tests to determine the effect of aerodynamic refinement on the drag characteristics of a conventional hull having a length-beam ratio of 9 (reference 3).

The present series of tests, conducted on a conventional hull of length-beam ratio of 6.7, were made to determine the effect on aerodynamic drag of systematic variations in the shape and disposition of the chines at and near the bow, in the depth of step, and in the chines rounded on both the forebody and afterbody hydrodynamic surfaces. The variations were made in such a manner that the results would indicate the importance of the drag of the bow, the step, and the sharp chines in relation to the over-all hull drag.

The "parent" form of the series was a hull modeled after that of a large, modern flying boat. The investigation was conducted in the Langley two-dimensional low-turbulence tunnel which is described in reference 4. All tests were made at a Reynolds number of 6.4×10^6 based on the hull length. Although some of the hull configurations investigated were impractical designs from hydrodynamic considerations, the tests were made to determine if the reduction in drag would be sufficiently large to warrant, for example, the incorporation of some auxiliary device such as a retractable step or retractable chines to produce a hydrodynamically practical hull.

SYMBOLS

C_L	lift coefficient $\left(\frac{L}{qS} \right)$
C_m	pitching-moment coefficient $\left(\frac{M}{qSc} \right)$
C_D	drag coefficient $\left(\frac{D}{qS} \right)$

C_{D_F}	frontal-area drag coefficient for hull including interference effect of mounting wing $\left(\frac{D_c - D_w}{qS_F} \right)$
α	angle of attack measured between wing chord and air stream, degrees
τ	angle of trim of hull measured between hull base and air stream, degrees
c	wing chord, feet
q	dynamic pressure, pounds per square foot $\left(\frac{1}{2} \rho V^2 \right)$
S	wing area, square feet
S_F	hull frontal area, square feet
R	Reynolds number based on model hull length
ρ	mass density of air, slugs per cubic foot
V	air velocity, feet per second
L	lift, pounds
M	pitching moment, foot-pounds
D	drag, pounds
Subscripts:	
c	wing-hull combination
w	wing alone

DESCRIPTION OF MODELS

The model had a normal depth of step equal to 8 percent of the beam and the length-beam ratio was 6.7. A three-view drawing of this basic model and a table giving model dimensions are shown in figure 1.

In order that changes in the model configurations could be easily made, the hull was assembled in 3 sections: the upper hull, the forebody hydrodynamic surfaces, and the afterbody hydrodynamic surfaces which also included the tail extension (fig. 1).

The offsets for the upper hull are given in table I. The dimensions of the canopy and a sketch illustrating the various hull dimensions are given at the end of the table.

Although the tests of the various forebodies were made primarily to detect the effect of changes in the chine lines near the bow, the keel shape was also modified in order that the series of bow shapes would be related and would represent practical hydrodynamic designs. The bow shapes investigated are shown in figure 2 and the offsets are presented in table II. The cross-sectional views at station 5.13 (fig. 2) are typical of the cross sections from the forward perpendicular to station 12.75. Each of the bow shapes had the same over-all plan form and was identical in cross section from station 12.75 to the step.

In order to maintain the same frontal area of the hull for all model configurations, the depth of step was varied by displacing the afterbody planing bottom vertically. The offsets for the various afterbodies thereby produced are presented in table III. Two of these afterbodies, the one used for the tests with 0 percent depth of step and the one used for tests with 16 percent (of the beam) depth of step, are shown in figure 3. This figure also shows that this method of varying the depth of step necessitated the refairing of the sides of the hull (see cross-sectional views at stations 33.75 and 41.25) and a part of the tail extension; but since the vertical sides are simply straight tangential lines connecting the chine and the upper hull, all afterbodies had comparable and related fairings. Some additional tests were made with an auxiliary longitudinal step attached to the forebody planing bottom, as shown in figure 4.

The offsets for the parent hull (model with 8 percent depth of step) with the forebody and afterbody chines rounded near the bow and sternpost, respectively, are presented in table IV and photographs of these chines are shown in figures 5(a) and 5(b). The offsets for the model with chines rounded over the entire forebody and afterbody hydrodynamic surfaces are presented in table V and photographs of this configuration (model with 0 percent of the beam depth of step) are presented in figures 5(c) and 5(d). The offsets for the afterbody (table V) also include ordinates for an afterbody fairing strip immediately aft of the step. This fillet is necessary to fair out the small step-like discontinuity in the chines that is caused by the added flare of the forebody planing bottom.

The wing was set at an incidence of 4.3° to the hull base line, had a chord of 14.08 inches, and was of the NACA 63,4-420 airfoil section (ordinates for airfoil given in table VI). The wing completely spanned the tunnel test section except for 0.03-inch gaps which were necessary to avoid fouling between the model and the tunnel walls.

A convenient method of designating the various model configurations was devised in order to simplify their identification throughout the rest of the paper. Since the parent hull model was derived from the offsets of Langley tank model 164, the same series number was retained as the first part of the designation for the present series of hulls. In the remaining part of the designation, the letters F and A followed by numbers designate the particular forebody and afterbody which was used to form the complete hull. The following table gives the basic model configurations which were investigated:

Model or hull designation	Model configuration	
	Forebody shape number	Depth of step (percent beam)
164-F1-A8	F1	8
^a 164-F2-A8	F2	8
164-F3-A8	F3	8
164-F4-A8	F4	8
164-F2-A0	F2	0
164-F2-A4	F2	4
164-F2-A12	F2	12
164-F2-A16	F2	16

^aParent hull.

Any modifications of the basic configurations are described with a statement; for example, "model 164-F2-A8 with chines rounded near the bow" or "model 164-F2-A4 with an auxiliary longitudinal step."

PROCEDURE AND TESTS

Since bow doors, turrets, and surface roughness would limit the extent of laminar flow over the wing and hull of a full-scale flying boat, transition strips of 0.01-inch carborundum grains were shellacked to the model to simulate the effect of such discontinuities in wing and hull contours. The transition strip on the hull (fig. 1) was located at a point 5 percent of the hull length aft of the bow of the hull and it was 0.50 inch in width. The transition strip on the wing, also shown in figure 1, covered the leading edge and the first 8 percent of both surfaces.

Lift, drag, and pitching-moment measurements were made on a three-component balance for the wing alone and for each of the wing-hull configurations. All the lift and the drag coefficients obtained from these tunnel tests were based on the model wing area of 3.52 square feet. The pitching-moment coefficients were based on the

wing chord of 1.173 feet. The drag coefficients of a given hull plus the wing-hull interference effects (hereinafter referred to simply as the drag of the hull) were obtained by subtracting, at any given angle of attack, the drag of the wing alone from the drag of the wing-hull combination. The drag coefficient for the hull was then converted from a coefficient based on the wing area to a coefficient based on the frontal area of 0.444 square foot.

The investigation was conducted in the Langley two-dimensional low-turbulence tunnel at a Reynolds number of 6.4×10^6 (based on the model hull length of 5.015 ft) which corresponded to a dynamic pressure of 53 pounds per square foot. Inasmuch as the corresponding Mach number of 0.19 was relatively low, no corrections for the effects of compressibility were applied to the data. All the aerodynamic characteristics were obtained over a range of hull trim angle from -10° to 10° , a considerably greater range of trim than is usually encountered by a full-scale flying boat.

TUNNEL CORRECTIONS AND ACCURACY OF DATA

The corrections for the wind-tunnel wall effects were made by the following equations:

$$q = 1.141q'$$

$$\alpha = 1.005\alpha'$$

$$C_L = 0.990C_L'$$

$$C_D = 0.995C_D'$$

$$C_M = 0.995C_M'$$

The constants which are used were obtained by the method described in reference 4 and the primed symbols represent the values measured in the tunnel.

The probable error in individual test points as determined from check tests, consideration of the sensitivity of the measuring instruments, and departure of points from the faired curves is estimated to be within the following limits:

Over the straight part of the lift curve:

C_L	±0.002
C_{D_F}	±0.0015
C_M	±0.001
α , deg	±0.03

Near maximum lift coefficient:

C_L	±0.008
C_{D_F}	±0.0048
C_M	±0.003
α , deg	±0.05

RESULTS AND DISCUSSION

The aerodynamic characteristics for the wing alone and for the wing with hull 164-F2-A8 (parent hull) are presented in figure 6 to show the changes in the lift, drag, and pitching-moment coefficients due to the presence of the hull. Similar lift, drag, and pitching-moment curves for the other configurations are not presented because no new effects are shown. The figure shows that the presence of the hull decreased the lift coefficients over the range of low to moderate angle of attack ($\alpha = 0^\circ$ to $\alpha = 8^\circ$) but increased the lift-curve slope and lift coefficients at angles of attack above 8.3° . This increase in lift and lift-curve slope at high angles of attack combined with the increase in the maximum lift coefficient obtained with the model of the wing-hull combination indicates in general that the presence of the hull had a favorable effect on the lift.

The addition of the hull to the wing causes the increment in drag coefficient to decrease as the angle of attack is increased in the positive direction. An examination of the tuft-survey sketches in figure 7 shows that the air flow over the wing-hull combination improves steadily as the attitude of the model is increased from low negative to high positive angles of attack. The higher lift-curve slope, the greater maximum lift coefficient, the smaller incremental rise in drag coefficient, and the smoother flow of air over the hull indicate that the wing-hull interference effects are favorable at these high angles of attack and that the hull has some lift. These favorable interference effects are shown by the occurrence in figure 8 of extremely low hull drag coefficients at relatively high hull trim angles. These favorable effects are obtained only for this one particular angle of incidence between the wing and hull, and similar results should not be expected if the angle of incidence is changed or if the wing is located at a different position on the hull.

An examination of the pitching-moment curves (fig. 6) shows that the addition of the hull to the wing increased the value of the negative pitching-moment coefficients at low to moderate lift coefficients but has little or no effect upon the pitching-moment coefficients at high values of the lift coefficient; thus, the addition of the hull apparently causes the pitching-moment curve to assume a positive or adverse slope.

Effect of bow shape on drag.— The effect of bow shape on the drag characteristics is presented in figure 9. An analysis of the results shows that at an angle of trim of -0.2° (the assumed trim angle of the hulls in high-speed level flight), hull 164-F1-A8 had the lowest drag coefficients of any of these hulls. Hull 164-F1-A8 had a slender bow incorporating a chine faired to conform more closely to the direction of the air flow at the bow. The reduction in drag coefficient obtained by use of this bow shape amounted to about 9 percent of the drag of hull 164-F2-A8 at this same trim angle. The drag coefficients of bow shapes F3 and F4 (hull 164-F3-A8 and hull 164-F4-A8, respectively) were approximately the same as the drag coefficient of 0.090 (at $\tau = -0.2^\circ$) which was obtained with hull 164-F2-A8. An examination of the curves at a trim angle of 1.7° (the assumed trim angle of the hulls for cruising speed in a level flight condition) shows that the drag coefficients obtained with all four of the bow shapes were about the same. Although variations in the lines of the chine have only a small effect on the over-all drag coefficient of a hull, some reduction in drag at the high-speed attitude can be realized by use of a chine of the type designated as "bow shape F1" in figure 2.

The effect of depth of step on drag.— An examination of the data (figs. 10 and 11) obtained with hulls 164-F2-A0, 164-F2-A4, 164-F2-A8, 164-F2-A12, and 164-F2-A16 shows that throughout the assumed range of trim for high-speed and cruising flight conditions, -0.2° to 1.7° , the greatest variations in the drag coefficients were obtained by decreasing the depth of step from 8 to 4 percent of the beam. Contrary to general belief, these results show that the drag coefficients within the flight range of trim do not vary proportionally with changes in the depth of step of the hull. The decrease in drag coefficient which was realized with hull 164-F2-A4 or hull 164-F2-A0 over that for hull 164-F2-A8 amounted to approximately 20 percent at the high-speed trim angle of -0.2° and to about 13 percent at the cruising-speed trim angle of 1.7° .

Although the lowest drag coefficients were usually obtained with hulls 164-F2-A4 and 164-F2-A0, they could not be used on an actual flying boat because normal ventilation of the step could not be obtained; and as a result the hulls would have excessive water resistance and very poor hydrodynamic stability characteristics. Results of hydrodynamic tests of several shallow step hulls (see p. 18 of reference 5) have shown, however, that satisfactory hydrodynamic stability characteristics could be obtained from such hulls provided that they were fitted with an auxiliary longitudinal step attached to the forebody immediately forward of the step. For this reason, the aerodynamic effects of adding an auxiliary longitudinal step to hull 164-F2-A4 were determined. These results are given in figure 12 and show that the auxiliary longitudinal step increased the drag of this hull by approximately 7 percent at both the high-speed trim angle of -0.2° and the cruising-speed trim angle of 1.7° . The drag coefficients of this modified hull were, however, still appreciably lower (about 14 percent at $\tau = -0.2^\circ$ and 6 percent at

$\tau = 1.7^\circ$) than those coefficients obtained with hull 164-F2-A8. Thus, the foregoing results indicate that a compromise arrangement consisting of an auxiliary longitudinal step and a shallow transverse step (4 percent of the beam) would provide the designer with an arrangement which would allow an appreciable reduction in aerodynamic drag without the hydrodynamic disadvantage of the shallow step.

The effect of rounded chines on the drag.— The results obtained from tests of hull 164-F2-A8 with the chines rounded near the bow and sternpost are presented in figure 13. An examination of the results shows that rounding only the forward part of the forebody chines (fig. 5(a)) reduced the drag coefficient of the parent hull by about 18 percent at a trim angle of -0.2° and by approximately 12 percent at a trim angle of 1.7° . The figure shows also that rounding the chines in the vicinity of the sternpost (fig. 5(b)) produced approximately the same reduction in the drag coefficient. Combining both of these modifications, however, gave no further decreases in drag within the experimental accuracy of the data. A comparison of these results with the data obtained for hulls 164-F2-A4 and 164-F2-A0 (fig. 10) shows that within the flight range of trim, rounding an appropriate part of the chines produced essentially the same reduction in drag coefficient that could be obtained by completely eliminating the step of a sharp chine hull. From these results it seems possible that a favorable aerodynamic-hydrodynamic compromise might be made, therefore, by rounding only the forward part of the forebody chines. Some form of a sharp, light-weight, retractable chine would, however, have to be incorporated into a hull of this shape to control the spray at low speeds when the hull acts as a displacement craft.

In order to determine the reduction in drag coefficients which could be obtained by completely eliminating the sharp chines, the step, and the chine flare of the forebody planing bottom, a series of tests were conducted on hull 164-F2-A0 shown in figures 5(c) and 5(d). The results obtained are presented in figure 14 together with the drag curve for the parent hull with sharp chines and for the hull with 0 percent depth of step and the sharp chines. The figure shows that the elimination of all sharp discontinuities decreased the drag coefficients of hull 164-F2-A0 throughout the entire range of trim which was investigated. A comparison of the drag coefficients obtained with hull 164-F2-A0 when all sharp discontinuities were removed with those drag coefficients obtained for the parent hull 164-F2-A8 shows that hull 164-F2-A0 produced drag coefficients which were about 30 percent lower at a trim angle of -0.2° and approximately 26 percent lower at a trim angle of 1.7° . An analysis of the results shows that at a trim angle $\tau = -0.2^\circ$, approximately one-third of the 30-percent reduction in drag is attributable to the elimination of the sharp chines and that the remaining two-thirds is attributable (see effects of changes in the depth of step on drag) to

elimination of the step. At a trim angle $\tau = 1.7^\circ$, one-half of the 26-percent reduction in drag is attributable to elimination of the chines and the remaining part is a result of eliminating the step. These test results serve to evaluate the gains that can be obtained with an idealized configuration which is very poor hydrodynamically. Any attempt to realize these drag gains on a practical flying boat would require the use of relatively complicated devices, such as retractable chines, retractable steps, and perhaps forced step ventilation to achieve good hydrodynamic characteristics.

Comparisons with other hulls and a body of revolution.— A comparison of the drag coefficients of several of the 164-series hulls with results obtained from tests of other hull forms and from tests of a streamline body of revolution (fineness ratio 5) are presented in figure 15. All the curves shown in this figure were obtained from tests with transition fixed near the bow of the models and all the coefficients include the interference effects of the mounting wing. The figure is intended to show the difference between the present hulls and the other hull forms and to bring out more clearly the reductions in drag coefficient which can be obtained by partly or completely eliminating the sharp chines and the transverse main step of a normal hull. It should be noted, however, that strict quantitative comparisons of the values obtained for the present hulls with those obtained for the other hull forms cannot be made because of the large differences in the Reynolds numbers and the great variation in the interference effects (see p. 9 of reference 6) which arise from the use of supporting wings of different chords, plan forms, and airfoil sections. An examination of the results obtained for the parent hull 164-F2-A8 and hull 213 (reference 1) shows that the drag of the parent hull was approximately 5 percent lower at $\tau = -0.2^\circ$ than the drag of hull 213, a similarly shaped hull of about the same length-beam ratio. Since the drag coefficient of the parent hull is lower for a lower value of the Reynolds number, the differences in the drag coefficients may be attributable to some slight differences in the initial degrees of aerodynamic cleanliness of the hulls and to the fact that the interference effects of the different supporting wings were probably more favorable for the case of the parent hull 164-F2-A8. A comparison at the same angle of trim shows that the drag coefficient of hull 164-F2-A8 was about 13 percent higher than the drag coefficient for the similarly shaped Hughes-Kaiser hull (reference 7) previously tested in the same tunnel. The greater part of this variation in drag is probably attributable to differences in the Reynolds number and to the type of mounting wing used; but some of this large difference in the drag is attributable to the fact that the Hughes-Kaiser hull, designed primarily for low drag, was a much cleaner hull from aerodynamic considerations.

These results presented in figure 15 show that the drag coefficient of 0.090 at $\tau = 0^\circ$ for hull 164-F2-A8 was about 77 percent greater (at the same trim angle) than the drag coefficient of 0.050 for the streamline body of revolution tested in reference 8. A comparison at the same angle of trim shows, however, that rounding a part of the forebody chines near the bow reduced the drag coefficient of hull 164-F2-A8 to a value of 0.073 which was only 46 percent higher than the drag coefficient obtained for the body of revolution.

If more radical changes in hull design such as the use of full-length retractable chines and retractable steps are acceptable, the drag of the hull of conventional shape can be reduced still further, as evidenced in figure 15, by the drag coefficient of 0.063 at $\tau = 0^\circ$ obtained for hull 164-F2-A0 when all sharp discontinuities were removed. This drag coefficient for the faired hull is still about 25 percent higher than the drag coefficient of the body of revolution, but is approximately the lowest drag that can be obtained from this type of hull without completely rounding the bottom or altering the shape of the tail extension. Since the greater part of the drag coefficient (fig. 15) of the body of revolution is skin-friction drag, any further sizable reductions in the drag of flying-boat hulls can be obtained only by reducing the amount of hull surface area.

SUMMARY OF RESULTS

An investigation, conducted at a Reynolds number of 6.4×10^6 based on hull length, was made to determine the effect on aerodynamic drag of systematic variations in the shape of a flying-boat hull. The parent hull was of conventional design (length-beam ratio equal to 6.7) and had a depth of step equal to 8 percent of the beam. An analysis of the results obtained at an angle of trim which corresponded to the assumed high-speed attitude of the hulls ($\tau = -0.2^\circ$) showed that:

1. The drag coefficient based on the hull frontal area of the parent hull was 0.090.
2. Although the variations in the lines of the bow in general had only a small effect on the drag coefficient of the hull, a reduction in drag equal to 9 percent of the drag of the parent hull could be obtained by using a slender bow (profile view) incorporating a chine faired to conform more closely to the direction of the air flow at the bow.

3. The drag coefficient for the hull with deep steps, 12 and 16 percent of the beam, was the same as that of the parent hull. The drag coefficient for the hull with a step depth equal to 4 percent of the beam was 20 percent less than that for the parent hull and complete elimination of the step, except for chine flare, produced no further reduction in drag.

4. A compromise arrangement consisting of an auxiliary longitudinal step and a shallow transverse step (4 percent of the beam) produced a hull which had 14 percent less drag than that of the parent hull and was believed to be hydrodynamically practical.

5. Rounding a part of the forebody or afterbody chines of the parent hull, either separately or together, produced the same (18 percent) decrease in the drag coefficient.

6. The elimination of all the sharp chines, the step, and the small discontinuity caused by the forebody chine flare reduced the drag coefficient of the parent hull by about 30 percent. One-third of this total reduction in drag is attributable to the elimination of the sharp chines whereas the remaining two-thirds is due to the elimination of the step.

Langley Memorial Aeronautical Laboratory
National Advisory Committee for Aeronautics
Langley Field, Va., November 18, 1947

REFERENCES

1. Yates, Campbell C., and Riebe, John M.: Effect of Length-Beam Ratio on the Aerodynamic Characteristics of Flying-Boat Hulls. NACA TN No. 1305, 1947.
2. Yates, Campbell C., and Riebe, John M.: Aerodynamic Characteristics of Three Planing-Tail Flying-Boat Hulls. NACA TN No. 1306, 1947.
3. Riebe, John M., and Naeseth, Rodger L.: Effect of Aerodynamic Refinement on the Aerodynamic Characteristics of a Flying-Boat Hull. NACA TN No. 1307, 1947.
4. von Doenhoff, Albert E., and Abbott, Frank T., Jr.: The Langley Two-Dimensional Low-Turbulence Pressure Tunnel. NACA TN No. 1283, 1947.
5. Berison, James M., and Bidwell, Jerold M.: Bibliography and Review of Information Relating to the Hydrodynamics of Seaplanes. NACA ACR No. 15G28, 1945.
6. Jacobs, Eastman N., and Ward, Kenneth E.: Interference of Wing and Fuselage from Tests of 209 Combinations in the N.A.C.A. Variable-Density Tunnel. NACA Rep. No. 540, 1935.
7. Fullmer, Felicien F., Jr.: Test of a 1/40-Scale Wing-Hull Model and a 1/10-Scale Float-Strut Model of the Hughes-Kaiser Cargo Airplane in the Two-Dimensional Low-Turbulence Pressure Tunnel. NACA MR, Sept. 24, 1943.
8. Becker, John V.: Wind-Tunnel Tests of Air Inlet and Outlet Openings on a Streamline Body. NACA ACR, Nov. 1940.

TABLE II
OFFSETS FOR THE VARIOUS BOW SHAPES

[All dimensions are given in inches]

Bow shape F1

Distance aft of station 0	1/2 max. beam	Chine above base line	Keel above base line	Buttock lines									
				0.25	0.50	0.75	1.00	1.25	1.50	1.75	2.00	2.50	3.00
^a -1.34	0.00	5.06	5.06										
-.84	.60	5.01	3.93	4.64	5.00								
-.42	.84	4.92	3.54	4.13	4.66	4.91							
0	1.03	4.80	3.24	3.76	4.25	4.63	4.80						
.38	1.19	4.66	3.00	3.48	3.95	4.36	4.60						
1.25	1.48	4.33	2.55	2.96	3.36	3.73	4.05	4.25					
2.25	1.76	3.96	2.14	2.49	2.83	3.17	3.47	3.71	3.88	3.95			
3.75	2.13	3.42	1.63	1.92	2.20	2.48	2.74	2.98	3.18	3.32	3.40		
5.13	2.41	2.95	1.26	1.50	1.74	1.97	2.20	2.41	2.60	2.75	2.87		
6.79	2.69	2.46	.93	1.12	1.31	1.50	1.69	1.87	2.03	2.17	2.30	2.45	
8.25	2.89	2.09	.71	.87	1.02	1.18	1.33	1.49	1.63	1.76	1.88	2.04	
9.75	3.04	1.78	.55	.67	.79	.93	1.05	1.18	1.30	1.42	1.53	1.70	1.78
11.25	3.16	1.56	.44	.55	.65	.76	.86	.97	1.08	1.18	1.28	1.45	1.55
12.75	3.25	1.40	.37	.46	.56	.65	.75	.84	.93	1.03	1.11	1.27	1.37
14.25	3.31	1.28	.31	.41	.50	.59	.68	.77	.86	.95	1.03	1.16	1.25
15.75	3.34	1.19	.26	.36	.45	.54	.63	.72	.81	.89	.96	1.09	1.18
17.25	3.37	1.12	.21	.30	.39	.48	.57	.66	.75	.83	.90	1.03	1.11
18.46	3.38	1.08	.17	.26	.35	.44	.53	.62	.70	.78	.85	.98	1.06
20.25	3.38	1.02	.11	.20	.29	.38	.47	.56	.64	.72	.79	.92	1.00
21.75	3.38	.97	.06	.15	.24	.33	.41	.50	.59	.67	.74	.86	.95
^b 22.75	3.38	.93	.02	.11	.20	.29	.38	.48	.56	.63	.70	.82	.91

Bow shape F2

Distance aft of station 0	1/2 max. beam	Chine above base line	Keel above base line	Buttock lines									
				0.25	0.50	0.75	1.00	1.25	1.50	1.75	2.00	2.50	3.00
^a -1.34	0.00	5.06	5.06										
- .84	.60	4.83	3.76	4.44	4.81								
- .42	.84	4.66	3.34	3.88	4.41	4.65							
0	1.03	4.49	3.02	3.51	3.99	4.34	4.49						
.38	1.19	4.34	2.77	3.23	3.67	4.06	4.28						
1.25	1.48	4.01	2.33	2.71	3.10	3.45	3.75	3.94					
2.25	1.76	3.66	1.95	2.27	2.59	2.92	3.20	3.43	3.59	3.65			
3.75	2.13	3.17	1.50	1.76	2.03	2.29	2.54	2.76	2.95	3.08	3.16		
5.13	2.41	2.77	1.18	1.40	1.63	1.85	2.06	2.26	2.44	2.58	2.69		
6.79	2.69	2.34	.88	1.07	1.24	1.43	1.61	1.78	1.93	2.07	2.19	2.33	
8.25	2.89	2.02	.69	.83	.98	1.14	1.29	1.44	1.57	1.70	1.81	1.98	
9.75	3.04	1.75	.54	.66	.78	.91	1.03	1.16	1.28	1.39	1.50	1.67	1.75
11.25	3.16	1.55	.44	.55	.65	.75	.86	.97	1.07	1.17	1.27	1.44	1.54
12.75	3.25	1.40	.37	.46	.56	.65	.75	.84	.93	1.03	1.11	1.27	1.37
14.25	3.31	1.28	.31	.41	.50	.59	.68	.77	.86	.95	1.03	1.16	1.25
15.75	3.34	1.19	.26	.36	.45	.54	.63	.72	.81	.89	.96	1.09	1.18
17.25	3.37	1.12	.21	.30	.39	.48	.57	.66	.75	.83	.90	1.03	1.11
18.46	3.38	1.08	.17	.26	.35	.44	.53	.62	.70	.78	.85	.98	1.06
20.25	3.38	1.02	.11	.20	.29	.38	.47	.56	.64	.72	.79	.92	1.00
21.75	3.38	.97	.06	.15	.24	.33	.41	.50	.59	.67	.74	.86	.95
^b 22.75	3.38	.93	.02	.11	.20	.29	.38	.48	.56	.63	.70	.82	.91

^aForward perpendicular.

^bStep.



TABLE II.- Concluded
 OFFSETS FOR THE VARIOUS BOW SHAPES - Concluded

[All dimensions are given in inches]

Bow shape F3

Distance aft of station 0	1/2 max. beam	Chine above base line	Keel above base line	Buttock lines									
				0.25	0.50	0.75	1.00	1.25	1.50	1.75	2.00	2.50	3.00
a-1.34	0.00	5.06	5.06										
- .84	.60	4.65	3.60	4.24	4.63								
- .42	.84	4.40	3.13	3.67	4.16								
.00	1.03	4.18	2.79	3.26	3.72	4.04	4.18						
.38	1.19	4.02	2.54	2.98	3.40	3.76	3.97						
1.25	1.48	3.69	2.10	2.47	2.84	3.17	3.45	3.62					
2.25	1.76	3.36	1.75	2.05	2.36	2.66	2.93	3.15	3.29	3.35			
3.75	2.13	2.93	1.37	1.61	1.86	2.09	2.33	2.54	2.72	2.85	2.91		
5.13	2.41	2.58	1.10	1.30	1.51	1.72	1.92	2.11	2.28	2.42	2.52		
6.79	2.69	2.22	.84	1.01	1.18	1.36	1.52	1.69	1.84	1.97	2.08	2.20	
8.25	2.89	1.95	.66	.80	.94	1.09	1.24	1.38	1.52	1.64	1.75	1.91	
9.75	3.04	1.72	.53	.65	.77	.89	1.01	1.13	1.25	1.36	1.47	1.63	1.72
11.25	3.16	1.54	.44	.54	.65	.75	.85	.96	1.06	1.16	1.27	1.43	1.53
12.75	3.25	1.40	.37	.46	.56	.65	.75	.84	.93	1.03	1.11	1.27	1.37
14.25	3.31	1.28	.31	.41	.50	.59	.68	.77	.86	.95	1.03	1.16	1.25
15.75	3.34	1.19	.26	.36	.45	.54	.63	.72	.81	.89	.96	1.09	1.18
17.25	3.37	1.12	.21	.30	.39	.48	.57	.66	.75	.83	.90	1.03	1.11
18.46	3.38	1.08	.17	.26	.35	.44	.53	.62	.70	.78	.85	.98	1.06
20.25	3.38	1.02	.11	.20	.29	.38	.47	.56	.64	.72	.79	.92	1.00
21.75	3.38	.97	.06	.15	.24	.33	.41	.50	.59	.67	.74	.86	.95
b22.75	3.38	.93	.02	.11	.20	.29	.38	.48	.56	.63	.70	.82	.91

Bow shape F4

Distance aft of station 0	1/2 max. beam	Chine above base line	Keel above base line	Buttock lines										
				0.25	0.50	0.75	1.00	1.25	1.50	1.75	2.00	2.50	3.00	
a-1.34	0.00	5.06	5.06											
-.84	.60	4.48	3.44	4.04	4.45									
-.42	.84	4.13	2.93	3.44	3.92									
.00	1.03	3.48	2.57	3.01	3.45	3.75	3.88							
.38	1.19	3.69	2.31	2.73	3.12	3.45	3.65							
1.25	1.48	3.36	1.88	2.23	2.58	2.89	3.15	3.30						
2.25	1.76	3.06	1.55	1.83	2.12	2.40	2.66	2.86	3.00					
3.75	2.13	2.68	1.24	1.45	1.68	1.90	2.12	2.33	2.49	2.61	2.67			
5.13	2.41	2.40	1.01	1.20	1.40	1.60	1.78	1.96	2.12	2.25	2.34			
6.79	2.69	2.10	.80	.95	1.12	1.28	1.44	1.60	1.74	1.87	1.97	2.08		
8.25	2.89	1.88	.64	.77	.91	1.05	1.19	1.33	1.46	1.58	1.69	1.84		
9.75	3.04	1.69	.53	.64	.76	.87	.99	1.11	1.22	1.33	1.43	1.60	1.69	
11.25	3.16	1.53	.44	.54	.64	.75	.85	.95	1.05	1.15	1.26	1.42	1.52	
12.75	3.25	1.40	.37	.46	.56	.65	.75	.84	.93	1.03	1.11	1.27	1.37	
14.25	3.31	1.28	.31	.41	.50	.59	.68	.77	.86	.95	1.03	1.16	1.25	
15.75	3.34	1.19	.26	.36	.45	.54	.63	.72	.81	.89	.96	1.09	1.18	
17.25	3.37	1.12	.21	.30	.39	.48	.57	.66	.75	.83	.90	1.03	1.11	
18.46	3.38	1.08	.17	.26	.35	.44	.53	.62	.70	.78	.85	.98	1.06	
20.25	3.38	1.02	.11	.20	.29	.38	.47	.56	.64	.72	.79	.92	1.00	
21.75	3.38	.97	.06	.15	.24	.33	.41	.50	.59	.67	.74	.86	.95	
b22.75	3.38	.93	.02	.11	.20	.29	.38	.48	.56	.63	.70	.82	.91	

a Forward perpendicular.

b Step.

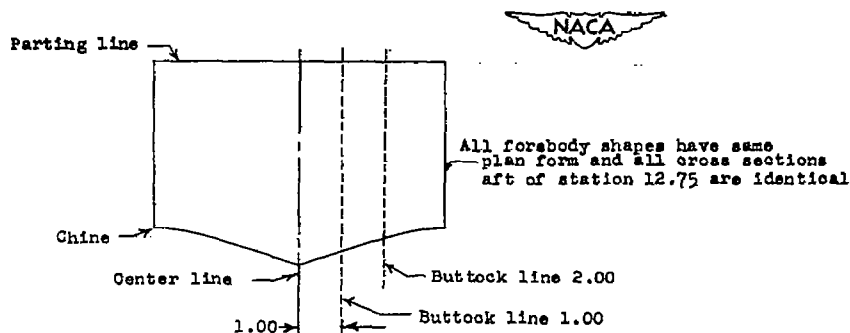


TABLE III

OFFSETS FOR THE VARIOUS AFTERBODY BOTTOM SHAPES

[All dimensions are given in inches]

Distance aft of station 0	Depth of step										Beam at chine
	0 inch (0 percent of beam)		0.27 inch (4 percent of beam)		0.54 inch (8 percent of beam)		0.81 inch (12 percent of beam)		1.08 inches (16 percent of beam)		
	A	B	A	B	A	B	A	B	A	B	
a22.75	0.02	1.25	0.29	1.52	0.56	1.79	0.83	2.06	1.10	2.33	3.38
23.25	.06	1.29	.34	1.56	.61	1.83	.88	2.10	1.15	2.37	3.37
24.75	.19	1.42	.47	1.69	.74	1.96	1.01	2.23	1.28	2.50	3.35
26.25	.33	1.54	.59	1.81	.87	2.08	1.14	2.35	1.41	2.62	3.31
27.75	.45	1.64	.73	1.91	1.00	2.18	1.27	2.45	1.54	2.72	3.24
29.25	.59	1.73	.86	2.00	1.13	2.27	1.40	2.54	1.67	2.81	3.13
30.75	.72	1.80	.99	2.08	1.26	2.35	1.53	2.62	1.80	2.89	2.99
32.25	.85	1.88	1.12	2.15	1.39	2.42	1.66	2.69	1.93	2.96	2.81
33.75	.98	1.93	1.26	2.20	1.53	2.47	1.80	2.74	2.07	3.01	2.58
35.25	1.11	1.96	1.38	2.23	1.65	2.50	1.92	2.77	2.19	3.04	2.32
36.75	1.25	1.98	1.52	2.25	1.79	2.52	2.06	2.79	2.33	3.06	2.00
38.25	1.38	1.98	1.65	2.25	1.92	2.52	2.19	2.79	2.46	3.06	1.65
39.75	1.51	1.96	1.78	2.23	2.05	2.50	2.32	2.77	2.59	3.04	1.25
41.25	1.65	1.94	1.92	2.21	2.19	2.48	2.46	2.75	2.73	3.02	.82
42.75	1.77	1.89	2.04	2.17	2.31	2.44	2.58	2.71	2.85	2.98	.33
b43.69	1.85	1.86	2.13	2.13	2.40	2.40	2.67	2.67	2.94	2.94	0
44.25	2.49		2.73		2.96		3.19		3.42		
45.75	3.92		4.05		4.17		4.30		4.43		
47.25	5.07		5.13		5.18		5.24		5.28		
48.75	5.95		5.96		5.97		5.98		5.99		
50.24	6.59		6.59		6.59		6.59		6.59		
51.75	7.07		7.07		7.07		7.07		7.07		

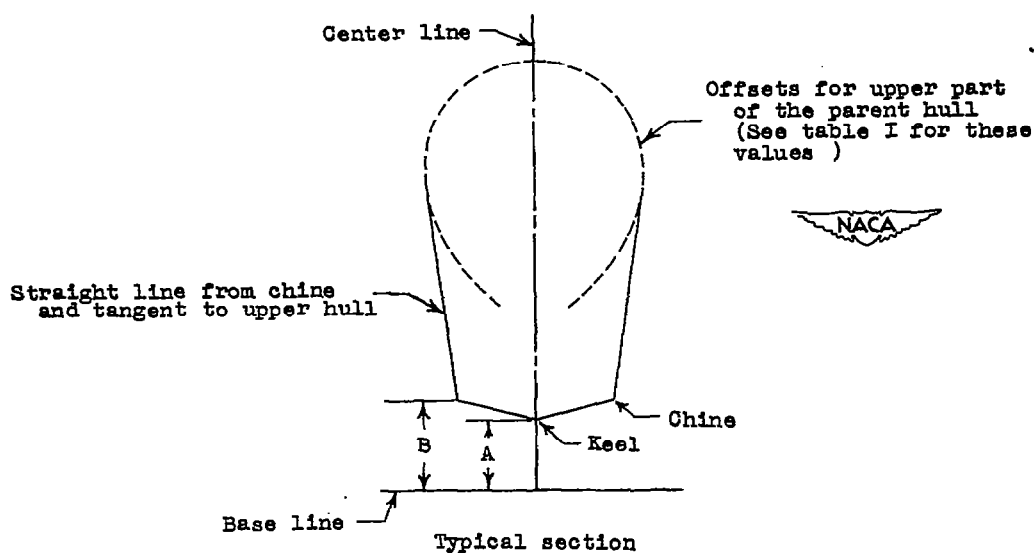
^aStep.^bSternpost.

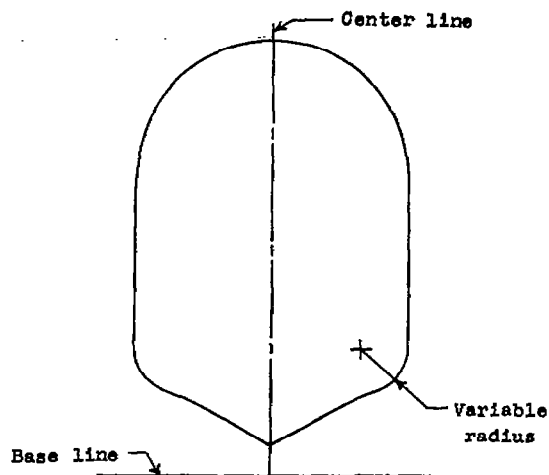
TABLE IV

OFFSETS FOR THE PARENT HULL WITH THE FOREBODY AND AFTERBODY ROUNDED NEAR THE BOW AND STERNPOST

[All dimensions are given in inches]

Forebody
(Bow shape F2)

Distance aft of station 0	Loc of centers and arc radii		
	Above base line	Out from center line	Radius of arc
^a -1.34			
-0.84	5.33	-0.40	1.00
-0.42	5.21	-.16	1.00
0	5.04	.04	1.00
.38	4.92	.19	1.00
1.25	4.61	.50	.99
2.25	4.27	.83	.95
3.75	3.78	1.33	.81
5.15	3.26	1.80	.60
6.79	2.67	2.33	.36
8.25	2.21	2.69	.19
9.75	1.85	2.95	.09
11.25			0
12.75	Sharp chines are maintained from station 11.25 to station 22.75		
14.25			
15.75			
17.25			
18.46			
20.75			
21.75			
^b 22.75			

^aForward perpendicular.^bStep.Afterbody
(Model with 8 percent depth of step)

Distance aft of station 0	Loc of centers and arc radii		
	Above base line	Out from center line	Radius of arc
^a 22.75	Sharp chines are maintained from station 22.75 to station 26.25		
23.25			
24.75			
26.25			
27.75	2.22	3.18	.06
29.25	2.41	2.96	.19
30.75	2.61	2.64	.36
32.25	2.84	2.27	.58
33.75	3.02	1.88	.76
35.25	3.14	1.52	.88
36.75	3.22	1.16	.96
38.25	3.26	.81	1.00
39.75	3.27	.44	1.00
41.25	3.25	.05	1.00
42.75	3.21	-.42	1.00
^b 43.69			1.00

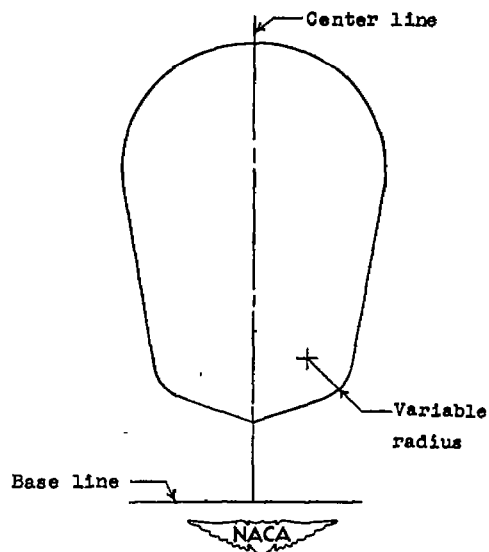
^aStep.^bSternpost.

TABLE V

OFFSETS FOR THE MODEL WITH 0 PERCENT DEPTH OF STEP AND WITH ALL DISCONTINUITIES REMOVED

[All dimensions are given in inches]

Forebody (Bow shape F2)			
Distance aft of station 0	Locus of arc centers		
	Above base line	Out from center line	Radius of arc
^a -1.34			
-.84	5.33	-0.40	1.00
-.42	5.21	-.16	1.00
0	5.04	.04	1.00
0.38	4.92	.19	1.00
1.25	4.62	.49	1.00
2.25	4.30	.77	1.00
3.75	3.89	1.14	1.00
5.15	3.55	1.42	1.00
6.79	3.15	1.70	1.00
8.25	2.84	1.89	1.00
9.75	2.58	2.05	1.00
11.25	2.37	2.16	1.00
12.75	2.24	2.25	1.00
14.25	2.15	2.31	1.00
15.75	2.08	2.35	1.00
17.25	2.03	2.37	1.00
18.46	1.98	2.38	1.00
20.25	1.91	2.38	1.00
21.75	1.86	2.38	1.00
^b 22.75	1.82	2.38	1.00

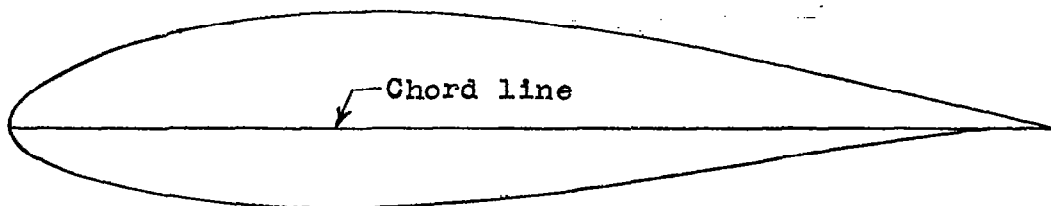
^aForward perpendicular.^bStep.

Afterbody (Model with 0 percent depth of step)									
Distance aft of station 0	Locus of arc centers			Buttock lines for chine fairing on afterbody					Chine above base line
	Above base line	Out from center line	Radius of arc	0.50	1.00	1.50	2.00	2.50	
^a 22.75	1.82	2.38	1.00	0.20	0.38	0.56	0.70	0.82	0.93
23.25	1.89	2.38	1.00	.25	.43	.60	.76	.89	1.05
24.75	2.10	2.36	1.00	.38	.56	.75	.92	1.09	1.35
26.25	2.24	2.26	1.00	.52	.70	.88	1.06	1.25	1.54
27.75	2.34	2.24	1.00	This fairing is necessary to fair out the chine flare of the forebody for this model configuration					
29.25	2.44	2.15	1.00						
30.75	2.52	2.02	1.00						
32.25	2.59	1.85	1.00						
33.75	2.64	1.64	1.00						
35.25	2.68	1.40	1.00						
36.75	2.71	1.11	1.00						
38.25	2.73	.79	1.00						
39.75	2.75	.41	1.00						
41.25	2.71	.01	1.00						
42.75	2.67	-.45	1.00						
^b 43.69			1.00						

^aStep.^bSternpost.

TABLE VI

ORDINATES FOR THE NACA 63,4-420 AIRFOIL			
[Stations and ordinates are given in percent airfoil chord]			
Upper surface		Lower surface	
Station	Ordinate	Station	Ordinate
0	0	0	0
.215	1.790	.783	-1.590
.430	2.196	1.070	-1.916
.887	2.827	1.613	-2.399
2.082	3.954	2.918	-3.210
4.538	5.557	5.462	-4.293
7.024	6.793	7.976	-5.097
9.526	7.817	10.474	-5.749
14.554	9.424	15.446	-6.732
19.603	10.589	20.397	-7.405
24.663	11.414	25.337	-7.834
29.732	11.895	30.268	-8.007
34.803	12.036	35.197	-7.916
39.874	11.906	40.126	-7.622
44.940	11.556	45.060	-7.176
50.000	11.025	50.000	-6.613
55.052	10.333	54.948	-5.953
60.095	9.492	59.905	-5.208
65.127	8.523	64.873	-4.403
70.148	7.438	69.852	-3.550
75.156	6.253	74.844	-2.673
80.150	4.990	79.850	-1.806
85.129	3.684	84.871	-.992
90.094	2.379	89.906	-.311
95.047	1.131	94.953	.133
100.000	0	100.00	0
L.E. radius: 3.16			
Slope of radius through L.E.: 0.168			



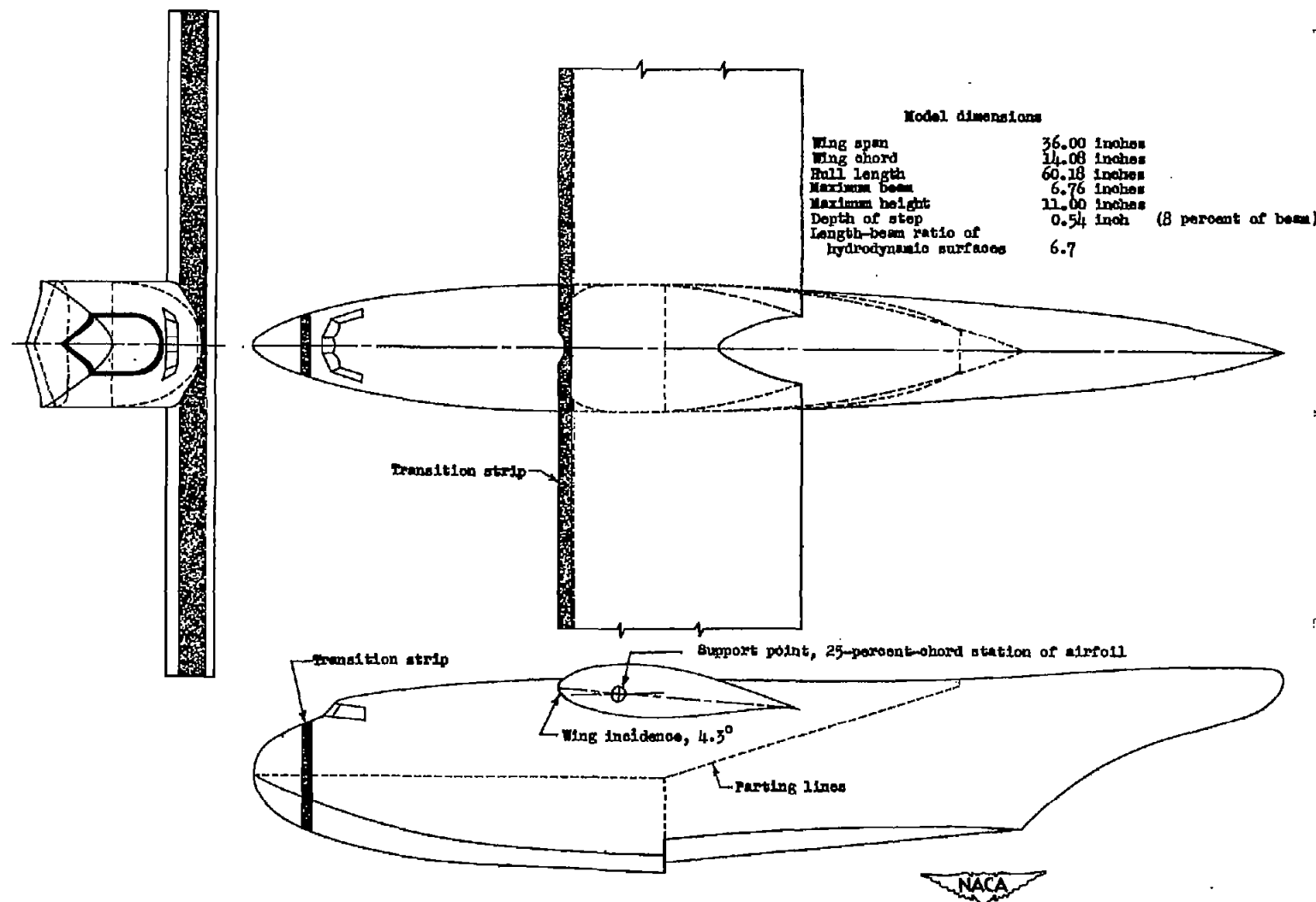


Figure 1.- Three-view drawing of parent wing-hull model.

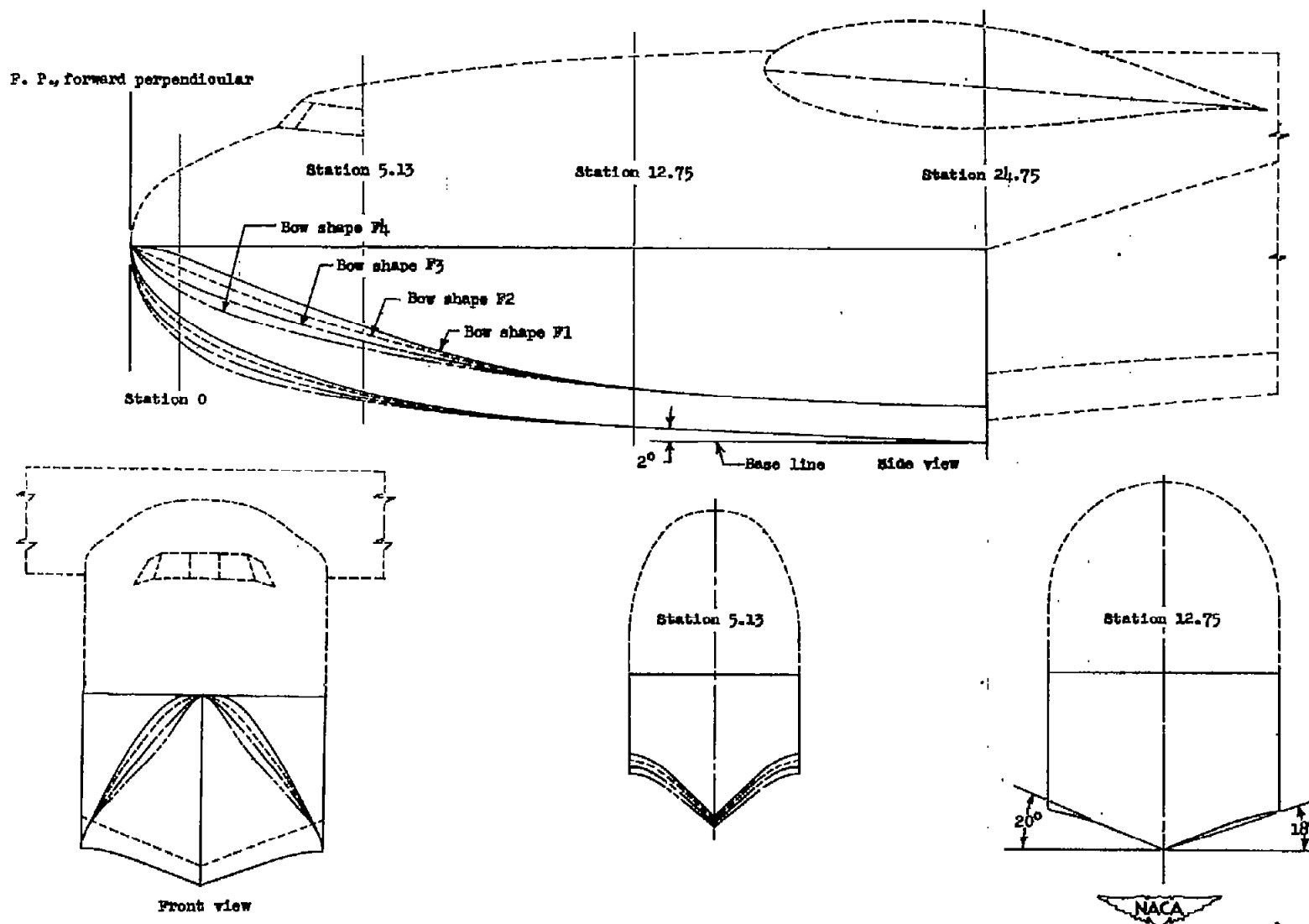


Figure 2.- Side, front, and sectional views of the various bow shapes.

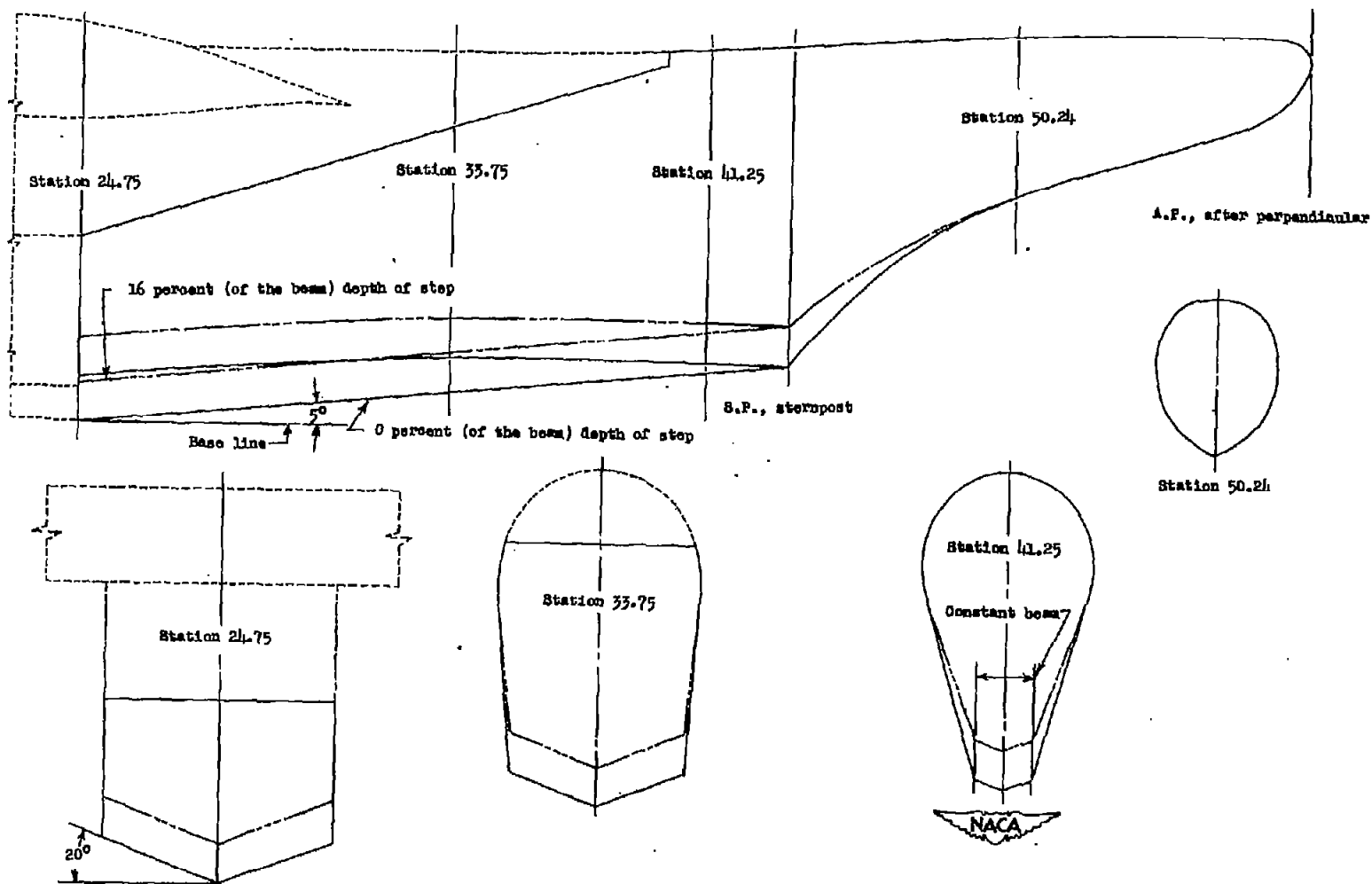


Figure 3.- Side and sectional views of the afterbodies for the models with 0 and 16 percent (of the beam) depth of step.

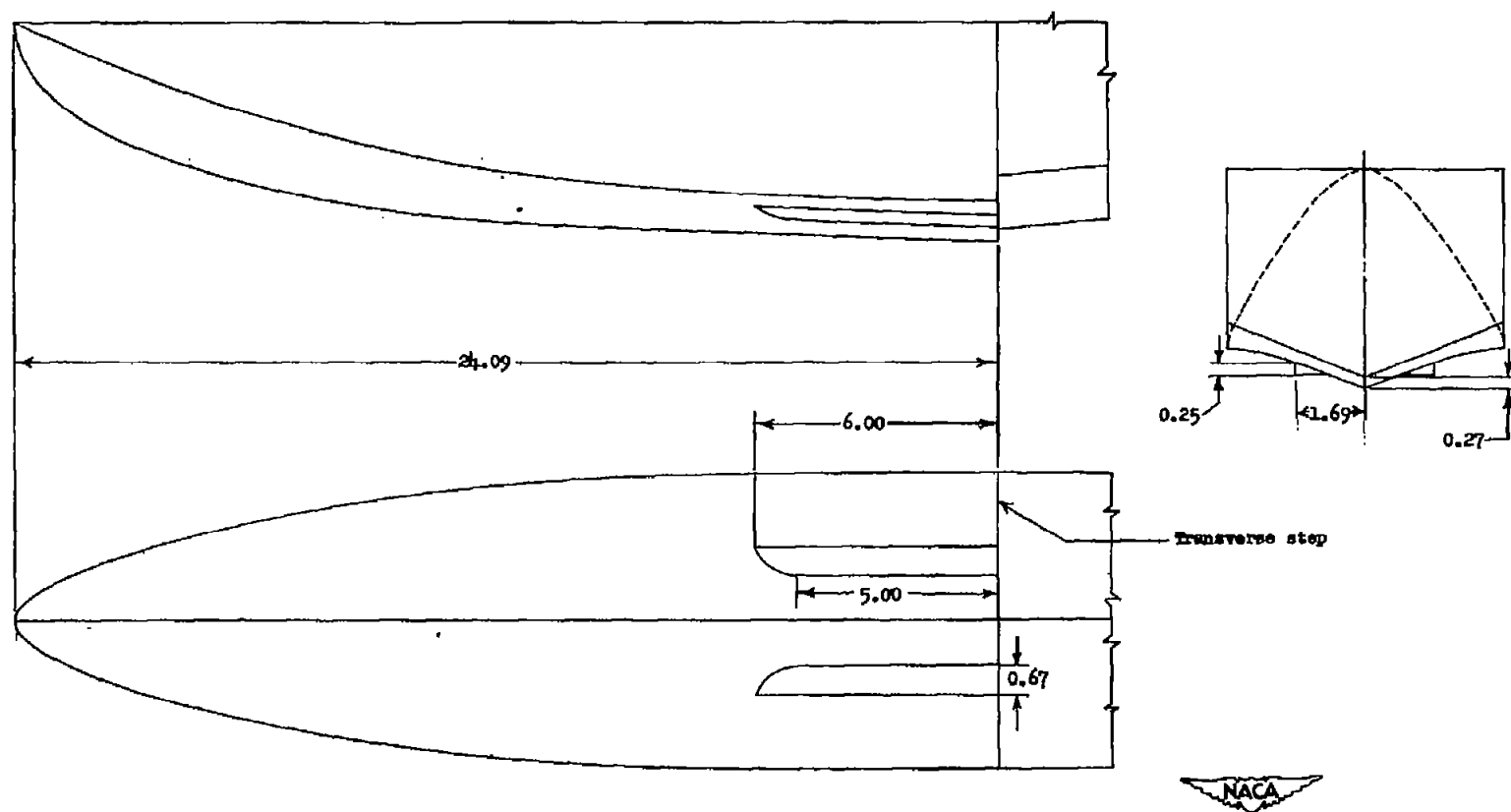
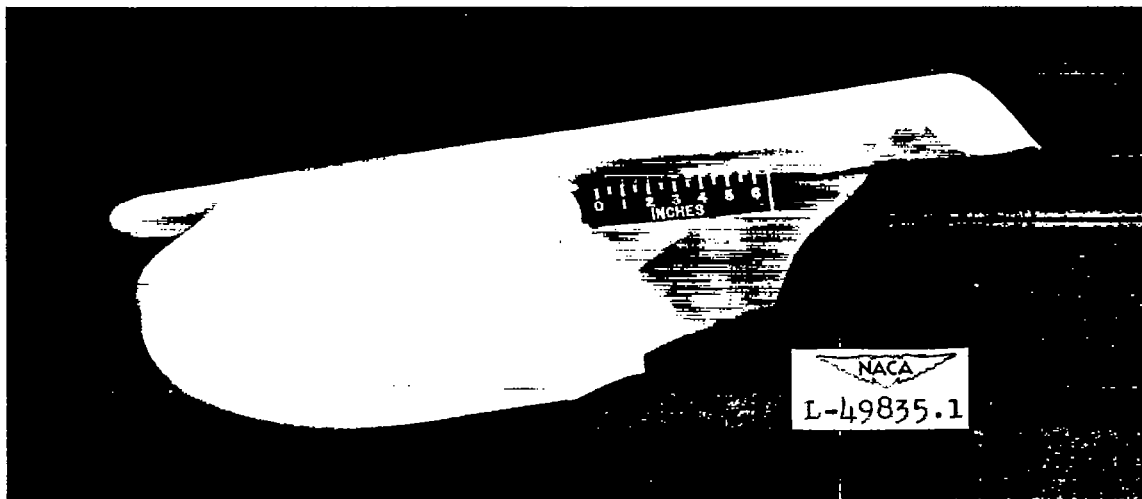


Figure 4.- The shape, location, and dimensions of the auxiliary longitudinal step as mounted on the model with 4 percent (of the beam) depth of step. (All dimensions are given in inches.)

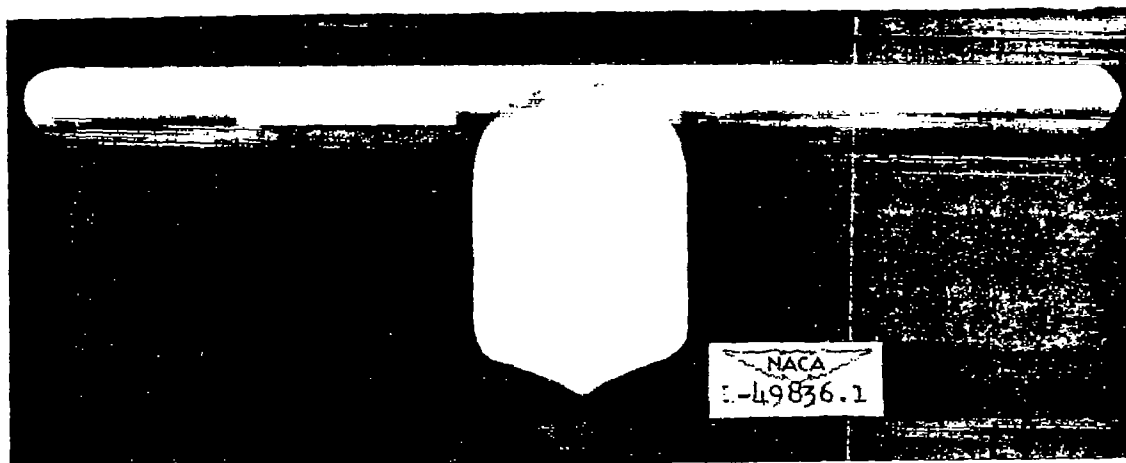


(a) Three-quarter front view of model 164-F2-A8 with chines rounded near the bow.

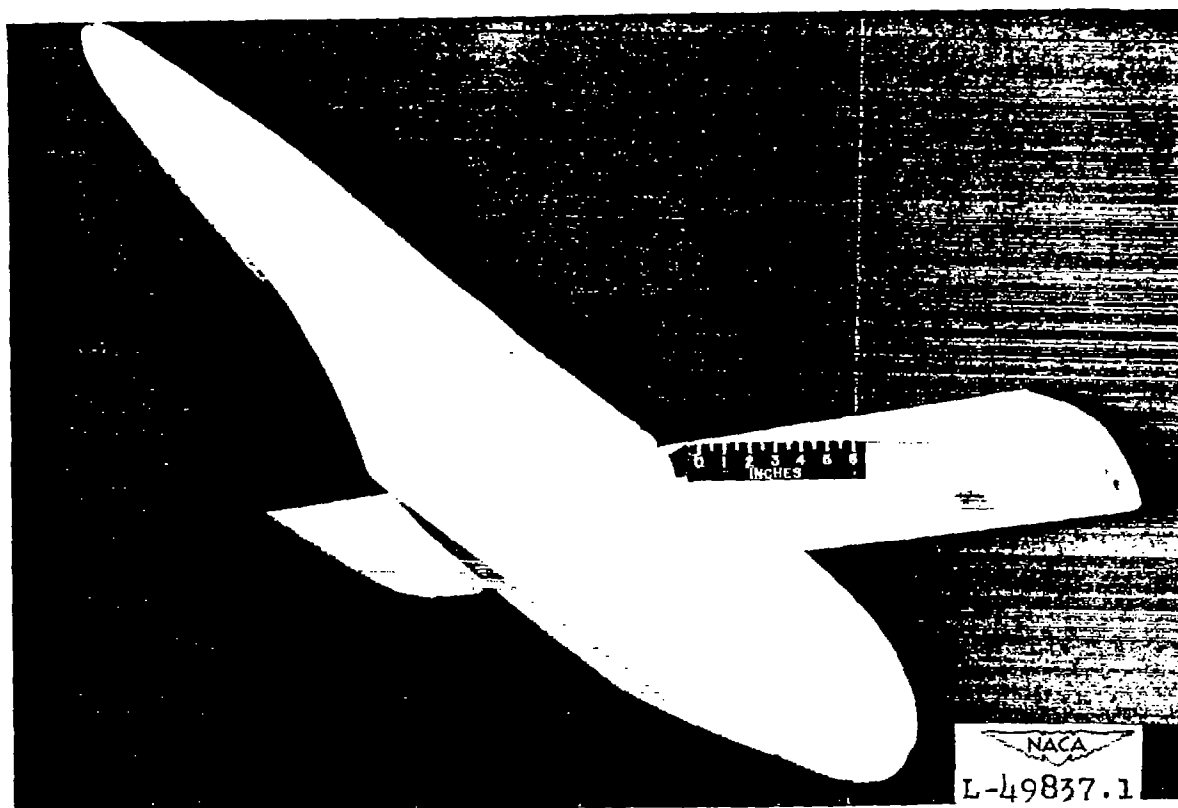


(b) Three-quarter rear view of model 164-F2-A8 with chines rounded near the sternpost.

Figure 5.- Photographs of the hulls with rounded chines.



(c) Front view of model 164-F2-A0 with all discontinuities removed.



(d) Three-quarter view of model 164-F2-A0 with all discontinuities removed.

Figure 5.- Concluded.

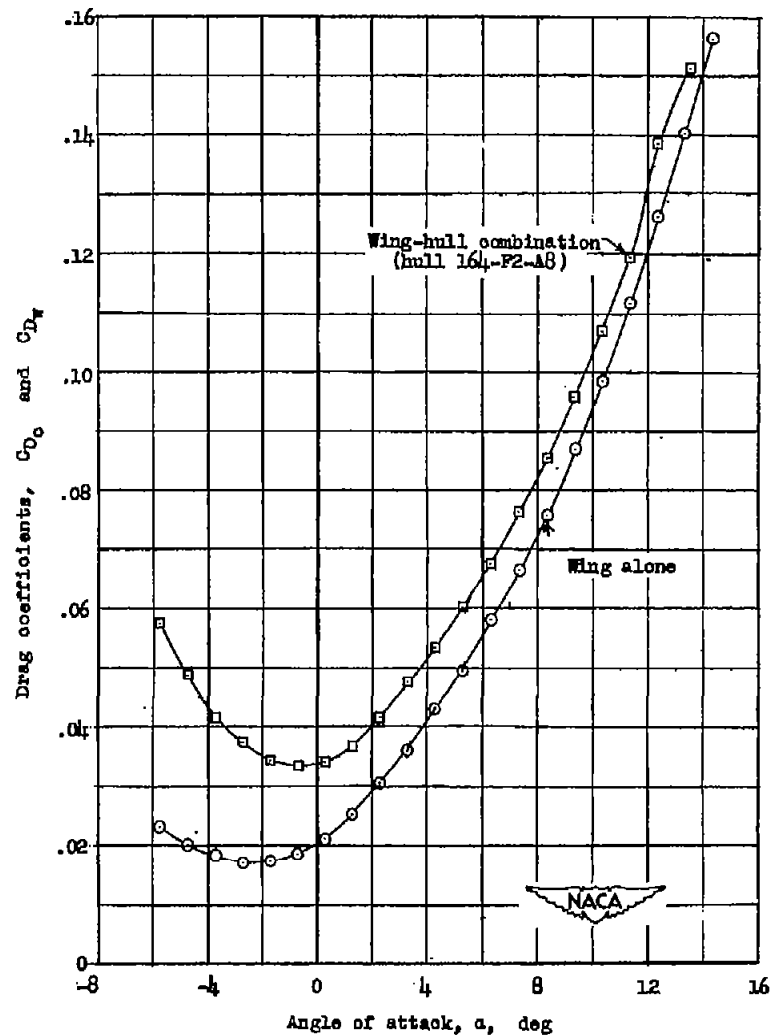
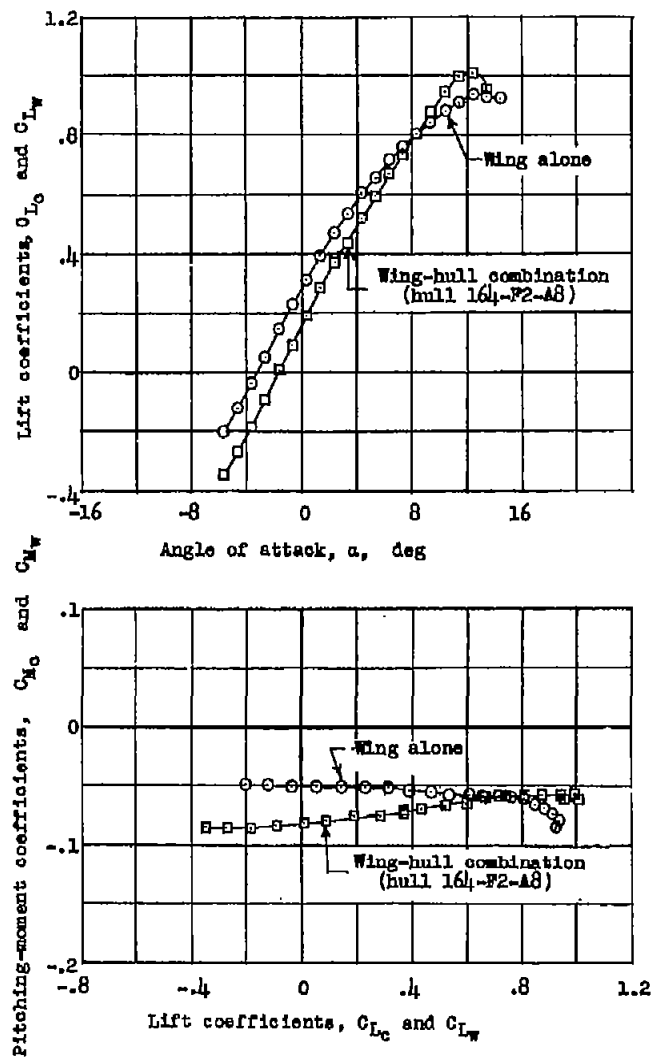


Figure 6.- Model lift, drag, and pitching-moment characteristics for the wing-hull combination (hull 164-F2-A8) and for the wing alone. $R = 6.4 \times 10^6$.

Steady flow \rightarrow Rough flow \rightarrow R Intermittently separated flow \rightarrow Separated flow \rightarrow

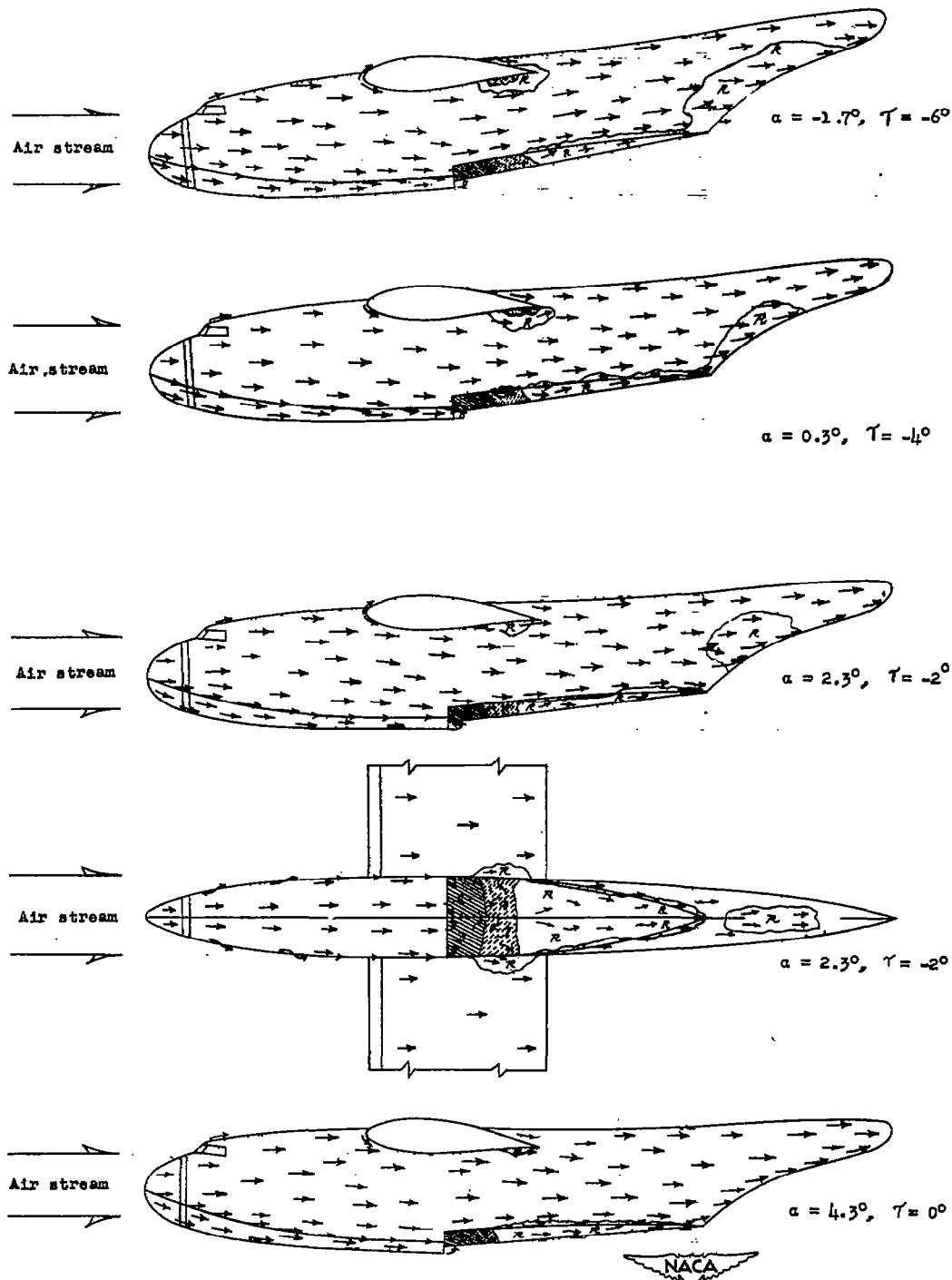




Figure 7.- Sketches showing the character of the air flow over the hull and wing of model 164-F2-A5.

Steady flow \rightarrow Rough flow $\leftarrow R$ Intermittently separated flow  Separated flow 

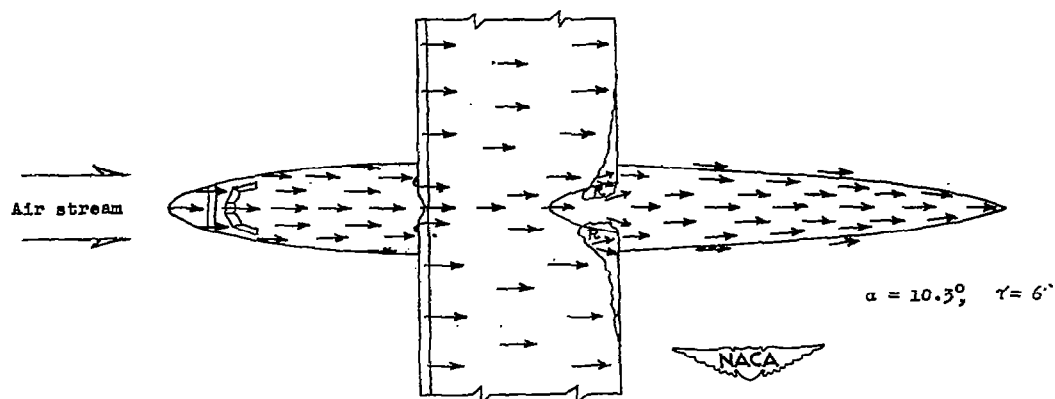
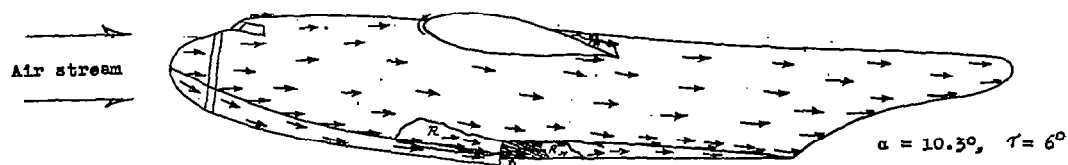
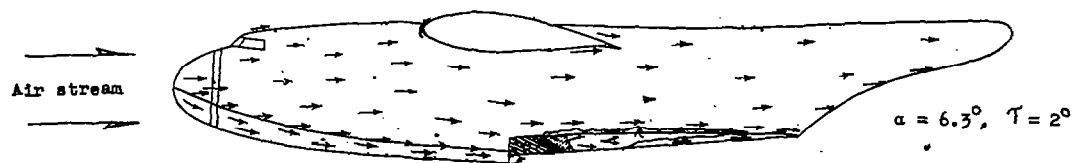




Figure 7.- Continued.

Steady flow \rightarrow Rough flow ∇R Intermittently separated flow  Separated flow 

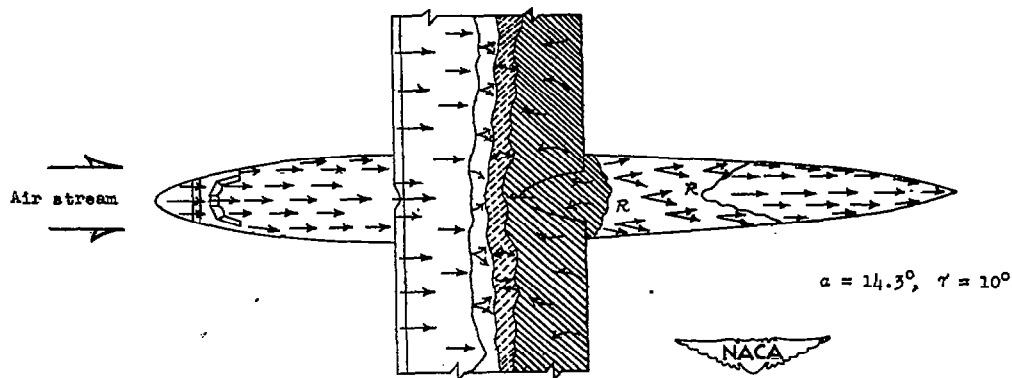
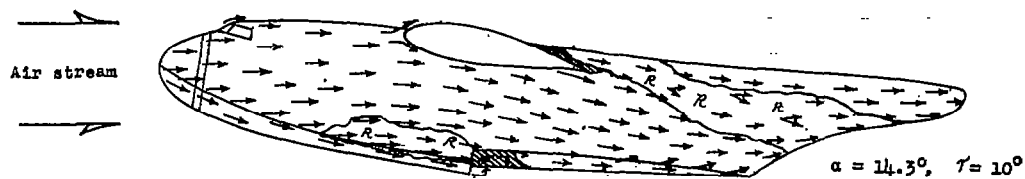
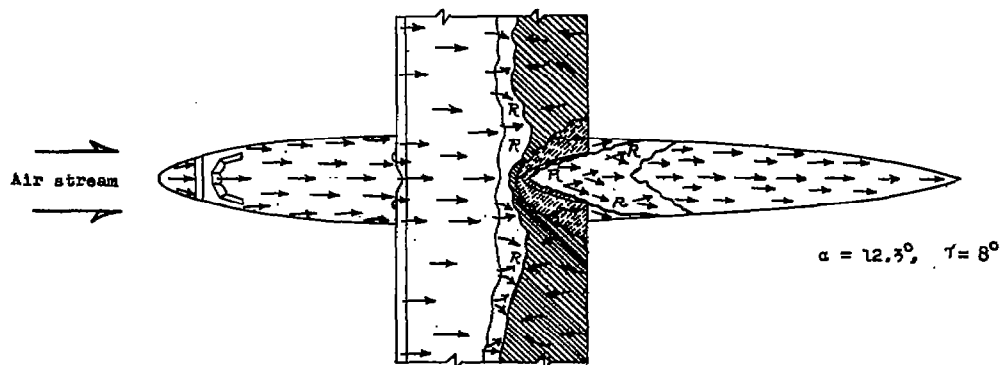
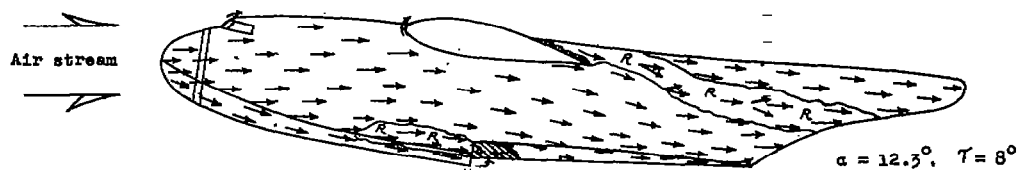


Figure 7.- Concluded.

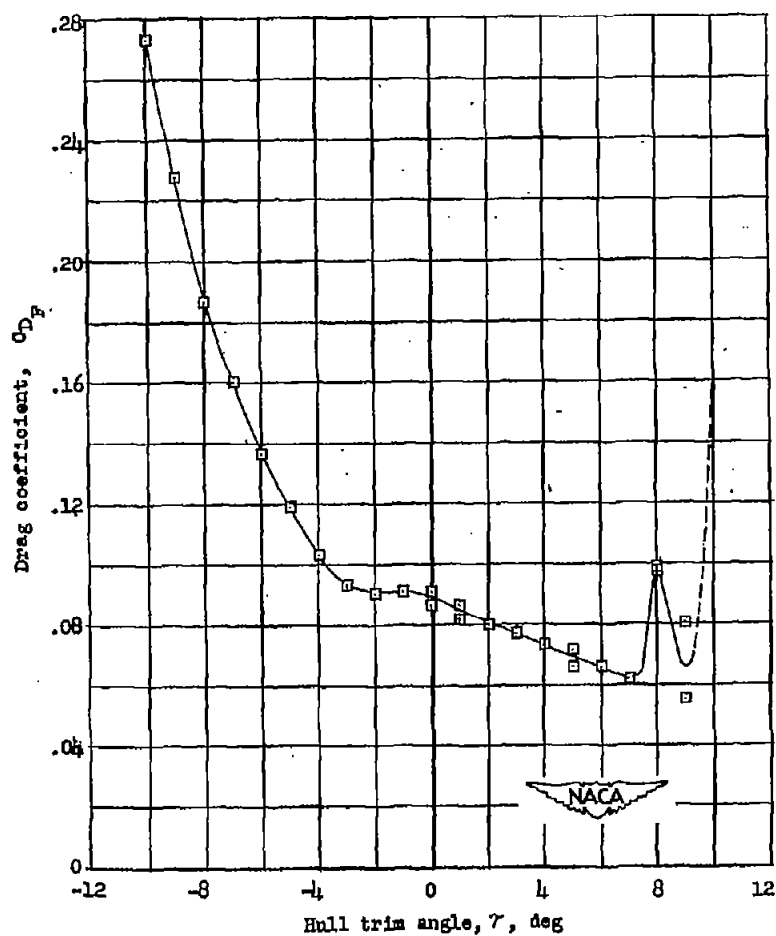


Figure 8.- Drag characteristics of the hull alone. Hull 164-F2-A8;
 $R = 6.4 \times 10^6$.

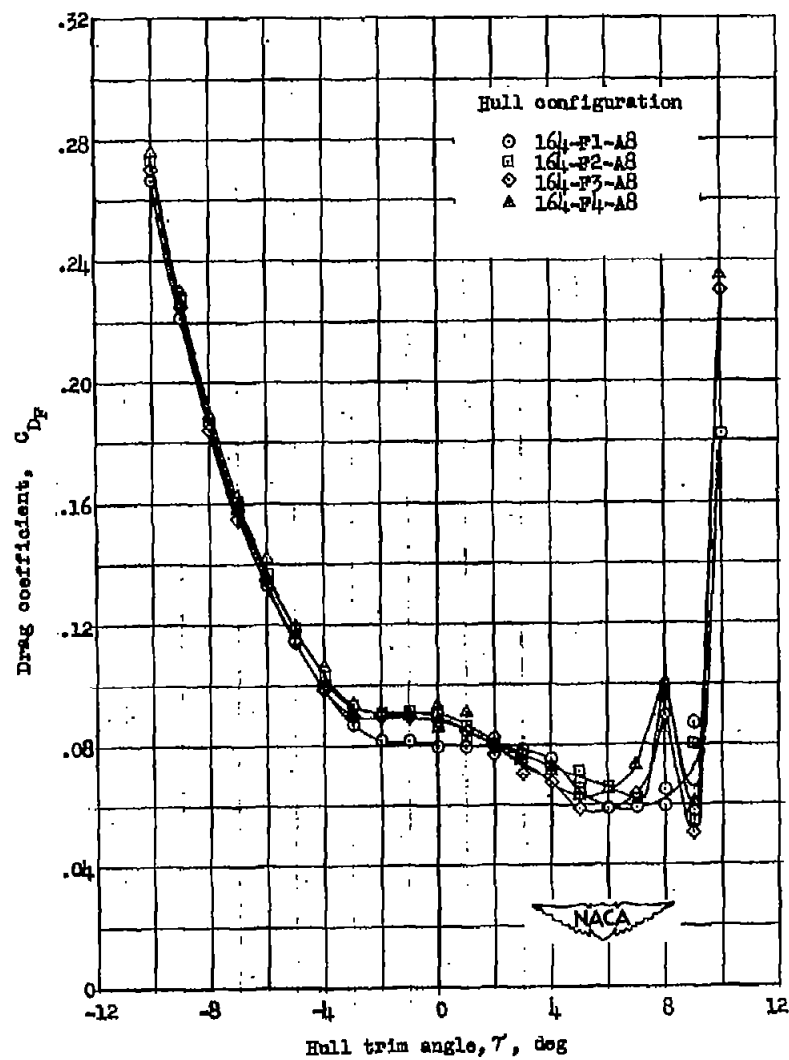


Figure 9.- The effect of bow shape on the drag characteristics
of the 164-series hulls. $R = 6.4 \times 10^6$.

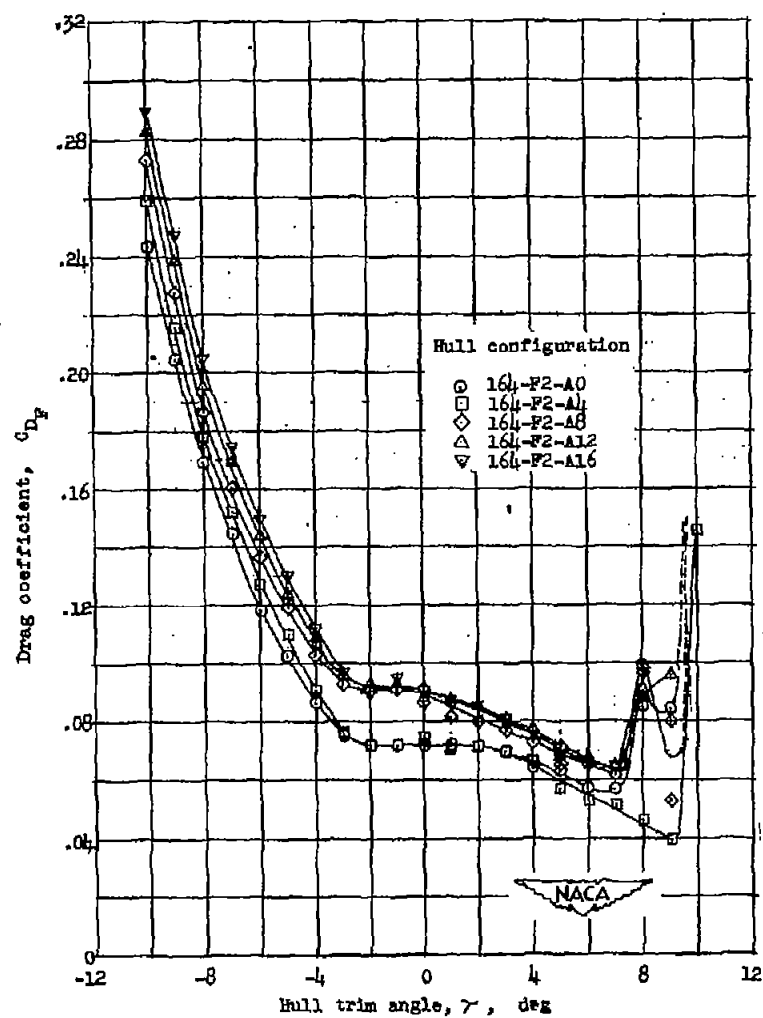


Figure 10.- The effect of step depth on the drag characteristics of the 164-series hulls. $R = 6.4 \times 10^6$.

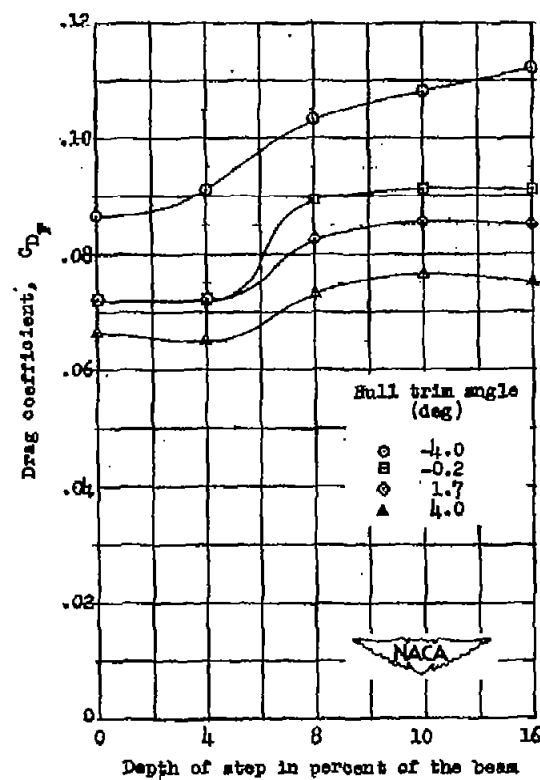


Figure 11.- The drag characteristics of the 164-F2 series hulls plotted as a function of the depth of step. $R = 6.4 \times 10^6$.

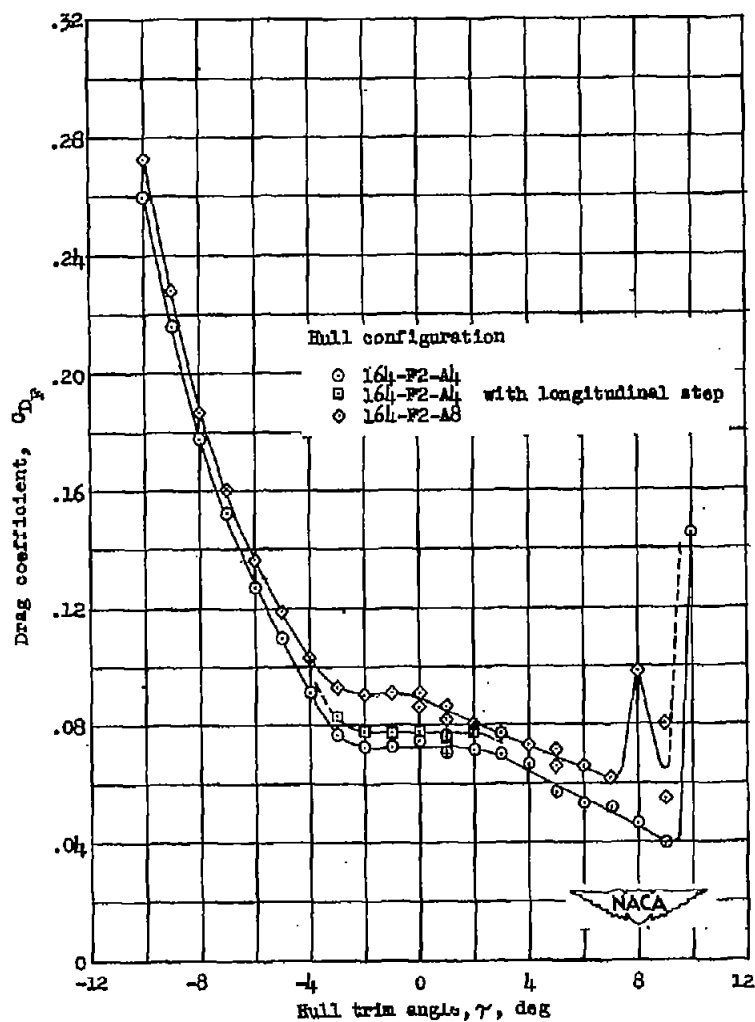


Figure 12.- The effect of an auxiliary longitudinal step on the drag characteristics of hull 164-F2-A4 and a comparison of the drag of this hull with that of hull 164-F2-A8. $R = 6.4 \times 10^6$.

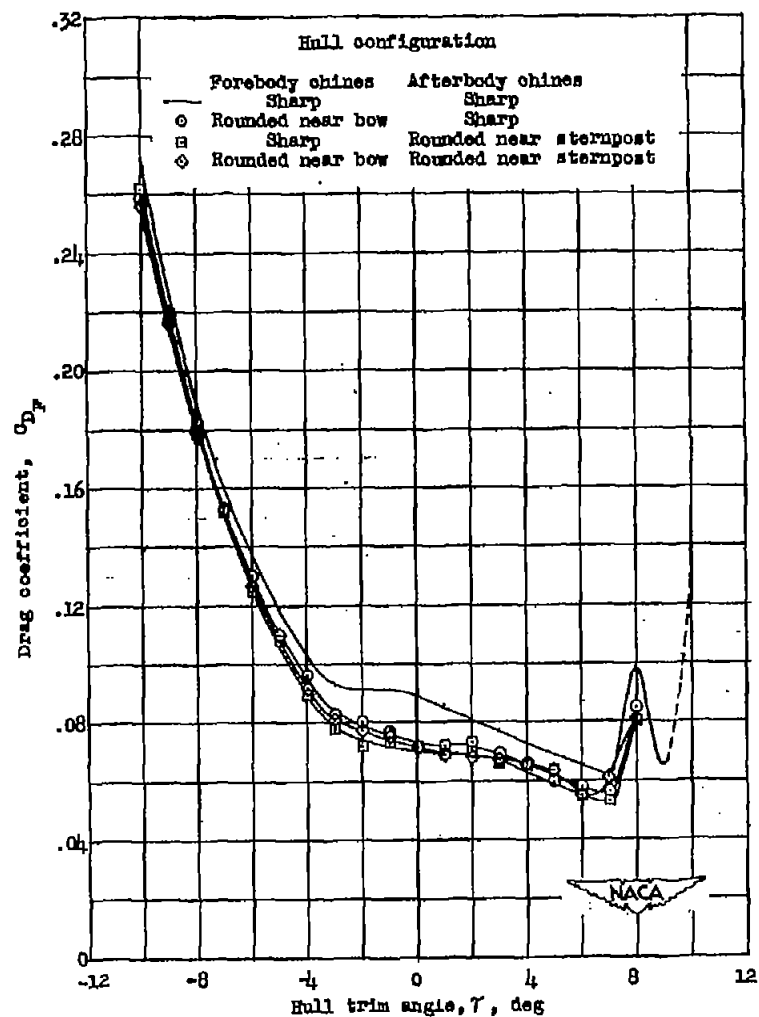


Figure 13.- The effect on the drag characteristics of rounding the chines near the bow and sternpost of hull 164-F2-A8. $R = 6.4 \times 10^6$.

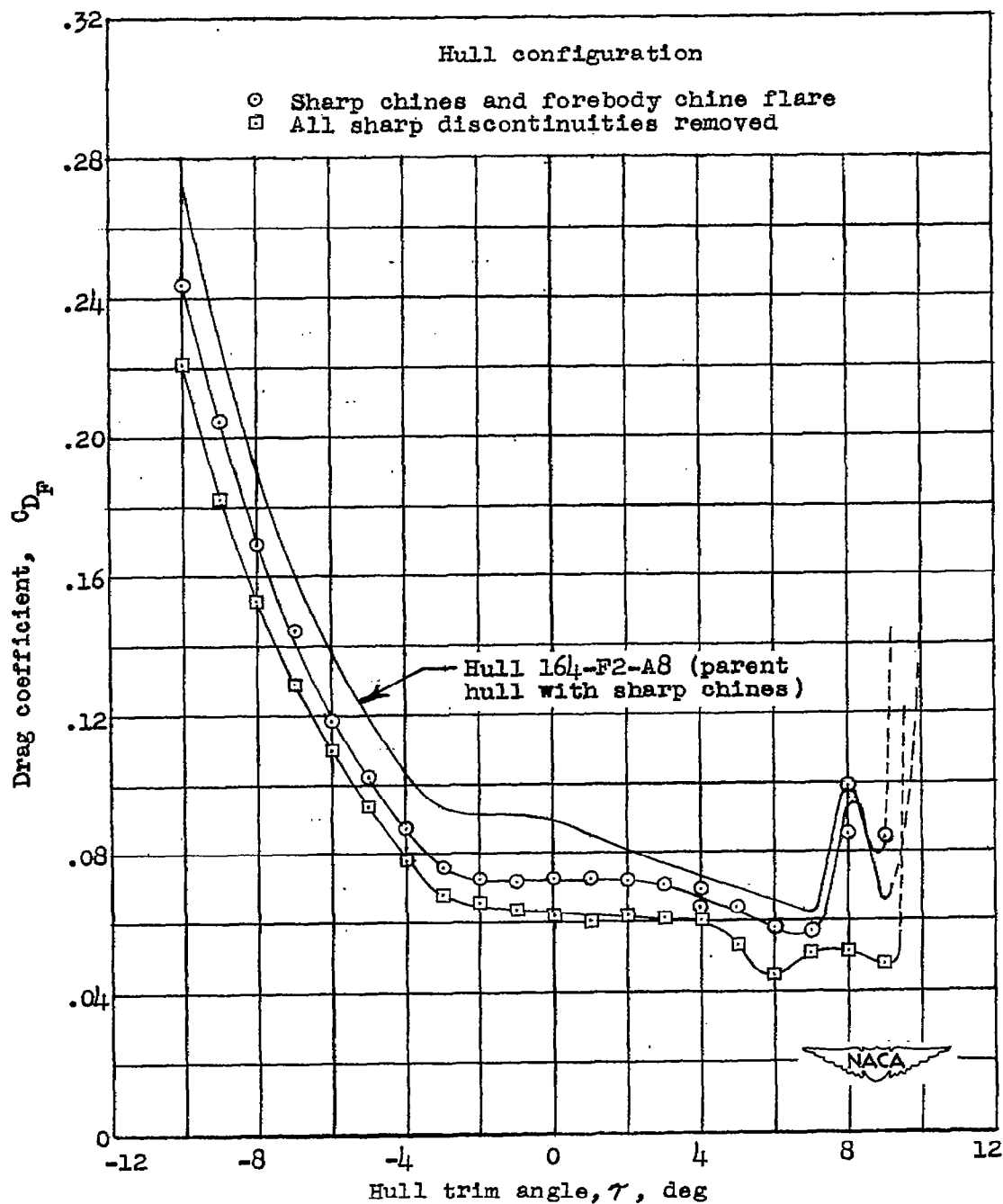


Figure 14.- The effect on the drag characteristics of eliminating all the sharp discontinuities on hull 164-F2-A0. $R = 6.4 \times 10^6$.

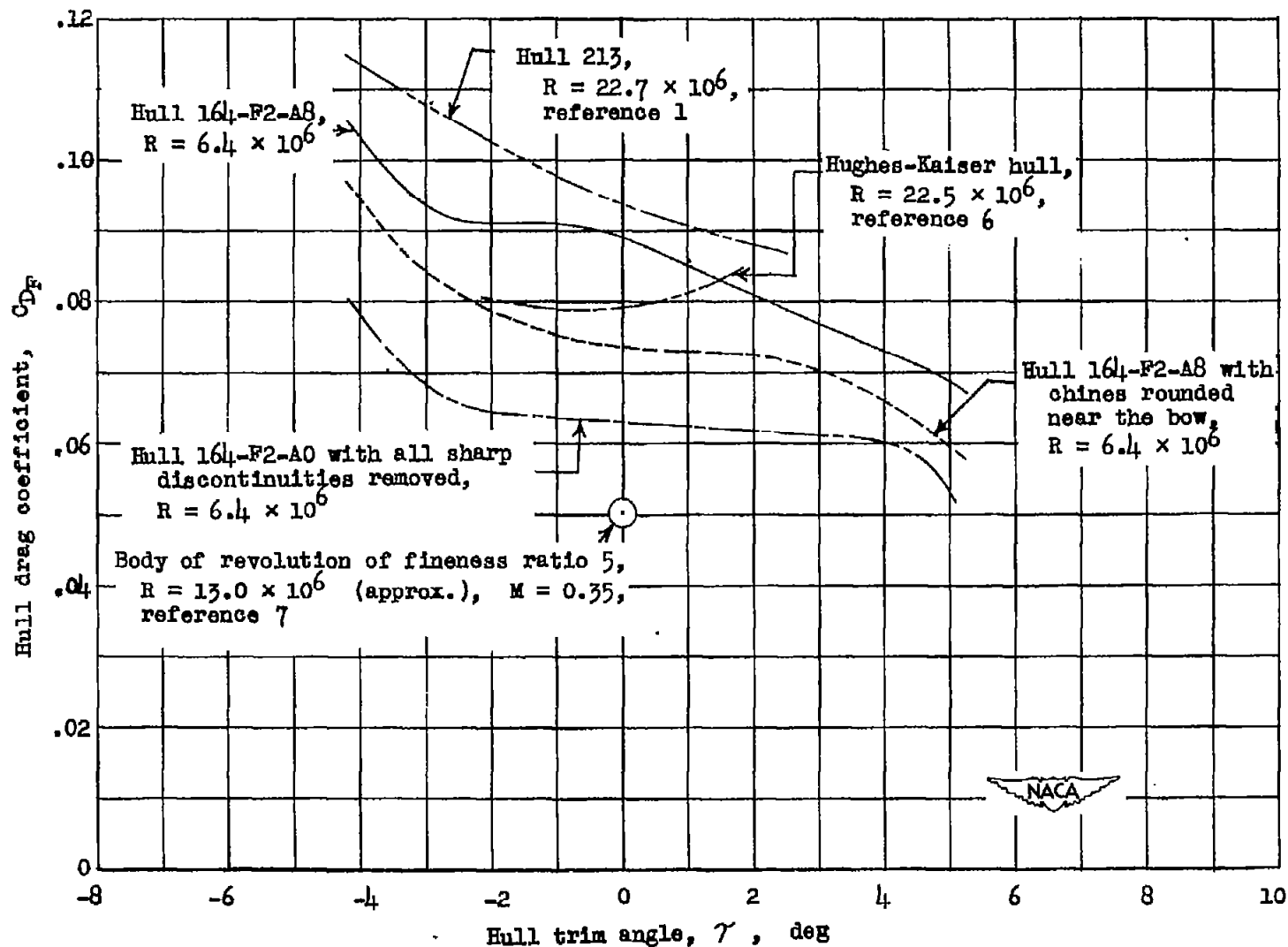


Figure 15.- The drag characteristics of several 164-series hulls as compared with other hull forms and a streamline body of revolution. Transition fixed near the bow of all hulls; Reynolds number based on hull length.